AIRS

ARIEL AIRS characterization of two infrared engineering grade detectors in the MWIR/LWIR band

Bataillon C., Pichon T., Amiaux J., Berthé M., Cara C., Cossou C., Horeau B., Kaszubiak G., Leguay N., Lortholary M., Provost L., Reboul B., Renaud D., Visticot F.

cnes cea cnrs

Plan

1. AIRS: ARIEL Infrared Spectrometer
    1. ARIEL space mission
    2. ARIEL spacecraft
    3. AIRS Acquisition chain architecture
2. Test bench at CEA
    1. Test bench presentation
3. Detector characterization results
    1. Strategy of calibration
    2. Detector baseline
    3. CDS and readout noise
    4. Dark current
    5. Readout glow
    6. Crosstalk
    7. Conversion gain and stability
4. Conclusion & Perspectives

Plan

1. AIRS: ARIEL Infrared Spectrometer
    1. ARIEL space mission
    2. ARIEL spacecraft
    3. AIRS Acquisition chain architecture
2. Test bench at CEA
    1. Test bench presentation
3. Detector characterization results
    1. Strategy of calibration
    2. Detector baseline
    3. CDS and readout noise
    4. Dark current
    5. Readout glow
    6. Crosstalk
    7. Conversion gain and stability
4. Conclusion & Perspectives

Atmospheric Remote-Sensing Infrared Exoplanet Large-survey

ARIEL is the M4 space mission of ESA to be launched in 2031.

ARIEL main goal is to go from exoplanets detection to exoplanets' atmosphere characterization.

Key questions addressed by ARIEL

What are the physical processes shaping planetary atmospheres ?

What are exoplanets made off ?

How do planets and planetary systems form and evolve ?

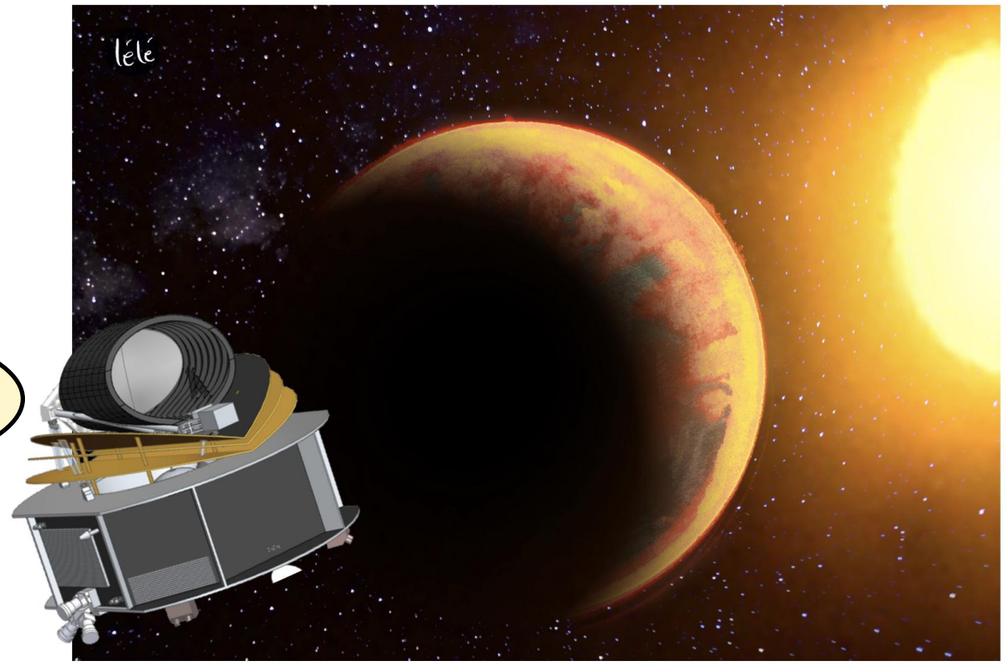

Ref. Redbook

Atmospheric Remote-Sensing Infrared Exoplanet Large-survey

ARIEL is the M4 space mission of ESA to be launched in 2031.

ARIEL main goal is to go from exoplanets detection to exoplanets' atmosphere characterization.

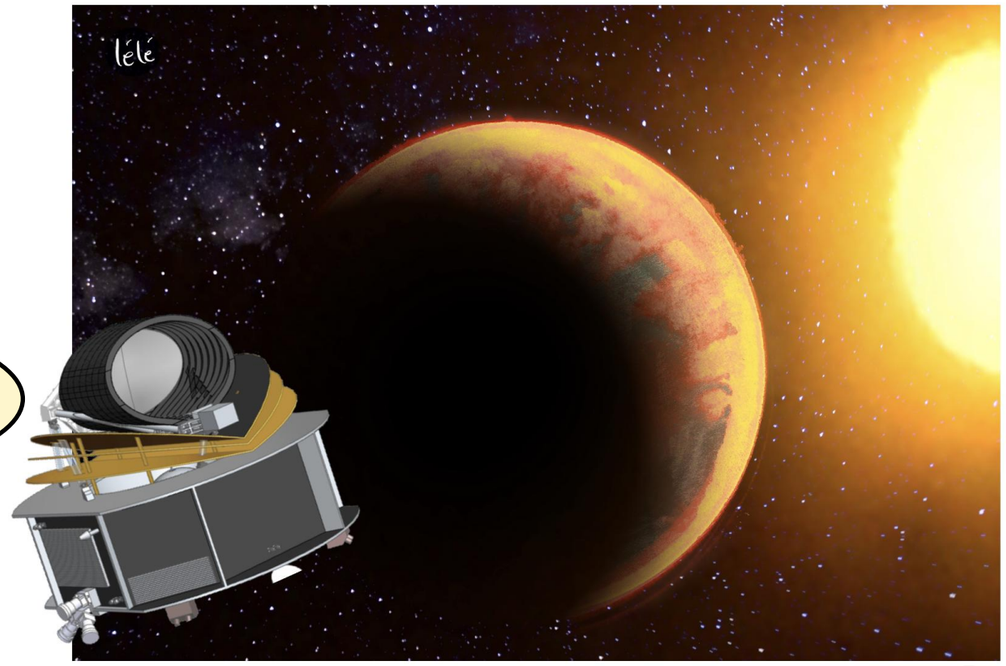

Key questions addressed by ARIEL

What are the physical processes shaping planetary atmospheres ?

What are exoplanets made off ?

How do planets and planetary systems form and evolve ?

Strategy:

→Around 1000 of diverse planets (mainly hot and warm planets) orbiting different types of stars.

→ Observational strategy : transit, eclipse and phase spectroscopy.

Underlying assumptions:

→Temporal variations of the measured signal can be attributed to changes in the small signal from the exoplanets and not result from variations of either the **instrument response** or of the **stellar activity.**

Requires extremely good acquisition chain stability

Monitored with visible photometry

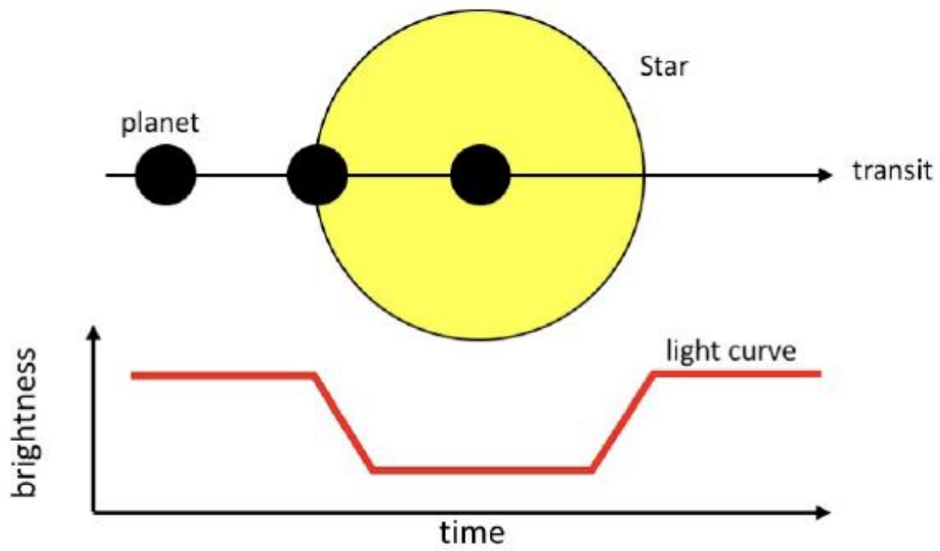

Schematic view of transit light curve

Ref. Redbook

1. AIRS: ARIEL Infrared Spectrometer
2. ARIEL spacecraft

1 meter class telescope of the ARIEL satellite

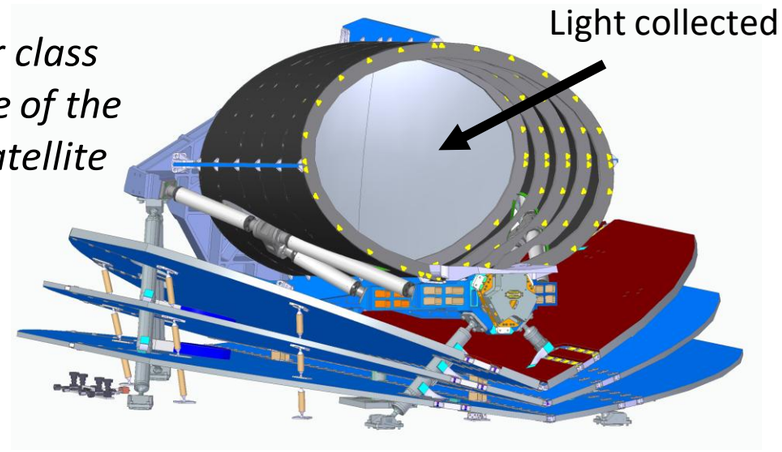

Front view of the PLM

AIRS: ARIEL InfraRed Spectrometer

FGS: Fine Guidance System

French contribution to ARIEL

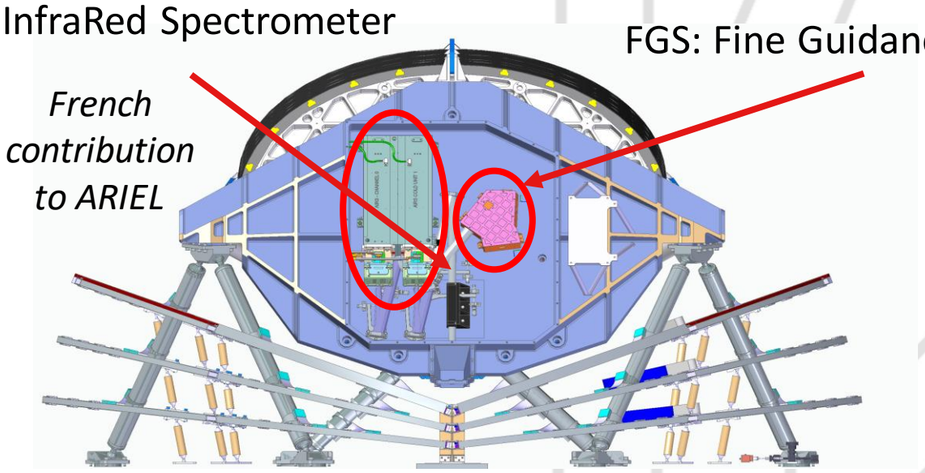

Rear view of the PLM

PLM : PayLoad Module
SVM : SerVice Module

1. AIRS: ARIEL Infrared Spectrometer
2. ARIEL spacecraft

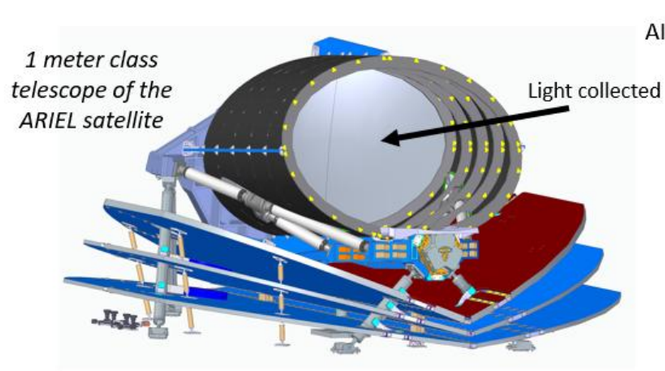

Front view of the PLM

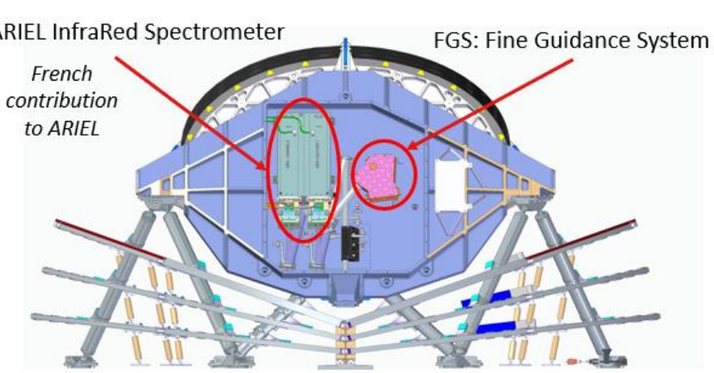

Rear view of the PLM

Simulated image acquired with AIRS instrument on the spectral band [3.9µm - 7.8µm] – CH1

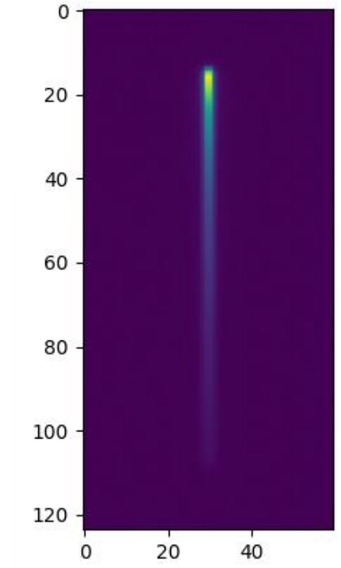

❖ **Ariel Infra-Red Spectrometer (AIRS)** instrument is composed of:

- Two optical channels with prisms dispersive elements: **CH0** covering the **[1,95-3,90]** µm range with R > 100 and **CH1** covering the **[3,90-7,80]** µm range with R>30
- Two Focal Planes with specific **Teledyne H1RG** detectors adapted to cut-off wavelength for CH0 and CH1
- Two detection chains with Cold Front End Electronics (CFEE) on the PLM and Detector Control Unit (DCU) on the SVM.

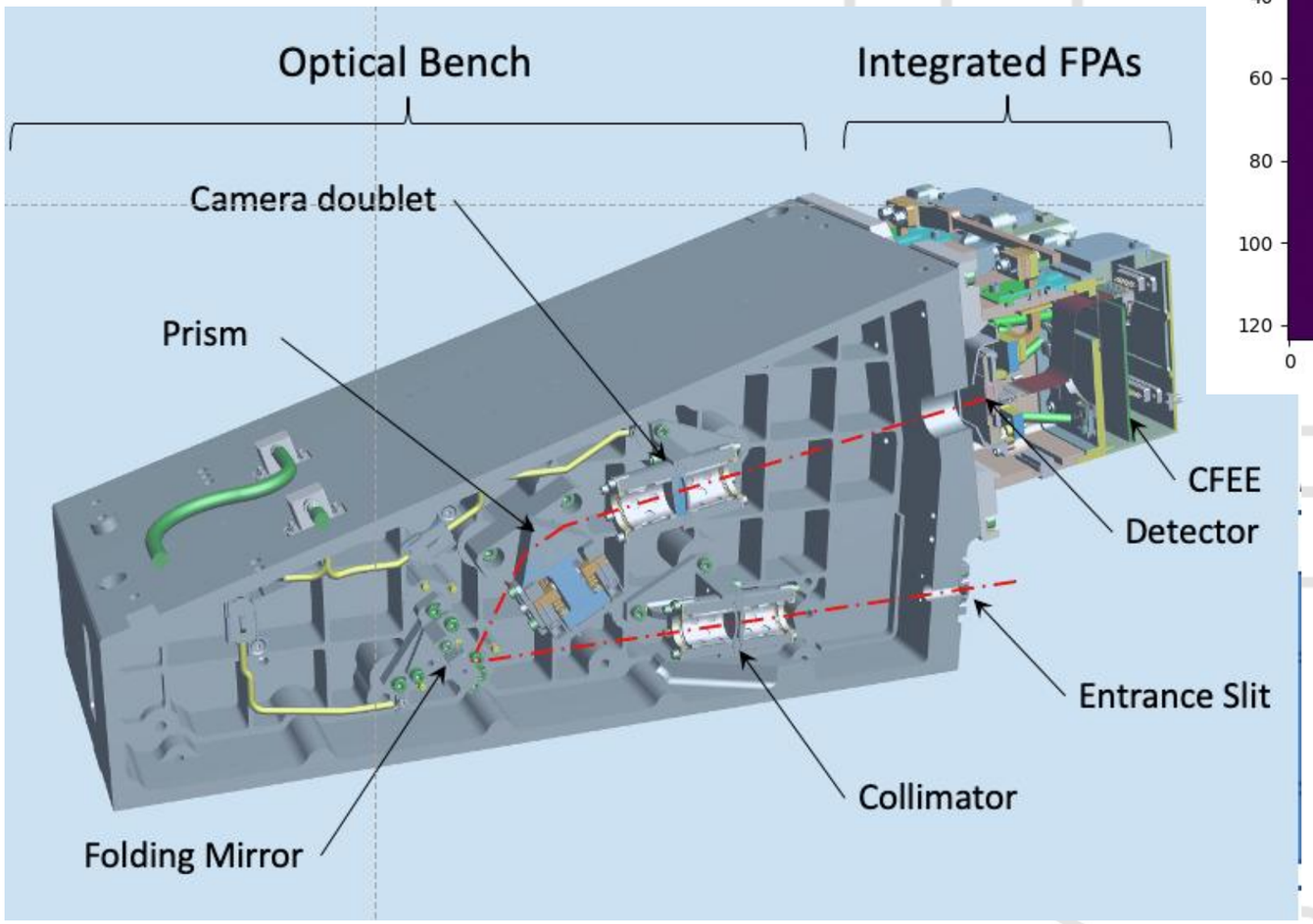

AIRS instrument : Optics Unit

PLM : PayLoad Module
SVM : SerVice Module

1. AIRS: ARIEL Infrared Spectrometer
2. ARIEL spacecraft

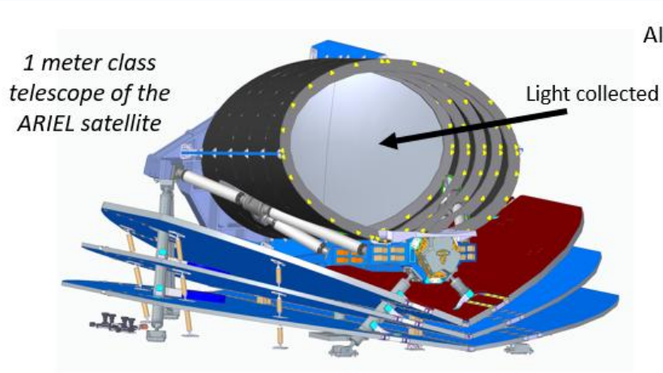

Front view of the PLM

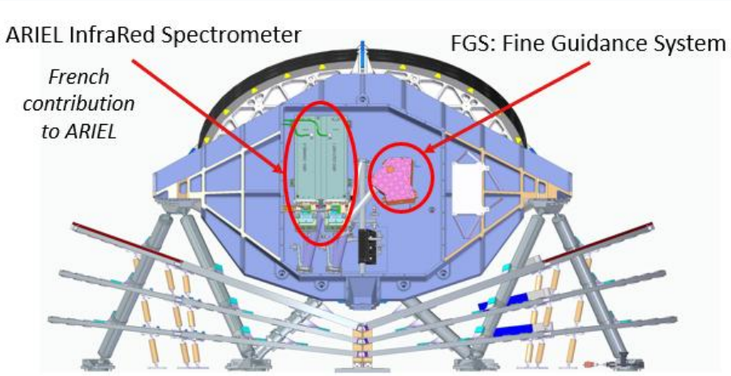

Rear view of the PLM

Simulated image acquired with AIRS instrument on the spectral band [3.9µm - 7.8µm] – CH1

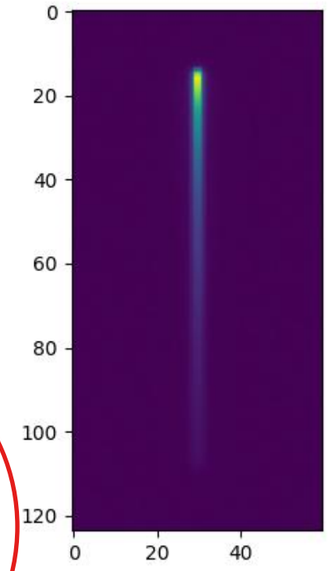

❖ **Ariel Infra-Red Spectrometer (AIRS)** instrument is composed of:

- Two optical channels with prisms dispersive elements: **CH0** covering the **[1,95-3,90]** µm range with R > 100 and **CH1** covering the **[3,90-7,80]** µm range with R>30
- Two Focal Planes with specific **Teledyne H1RG** detectors adapted to cut-off wavelength for CH0 and CH1
- Two detection chains with Cold Front End Electronics (CFEE) on the PLM and Detector Control Unit (DCU) on the SVM.

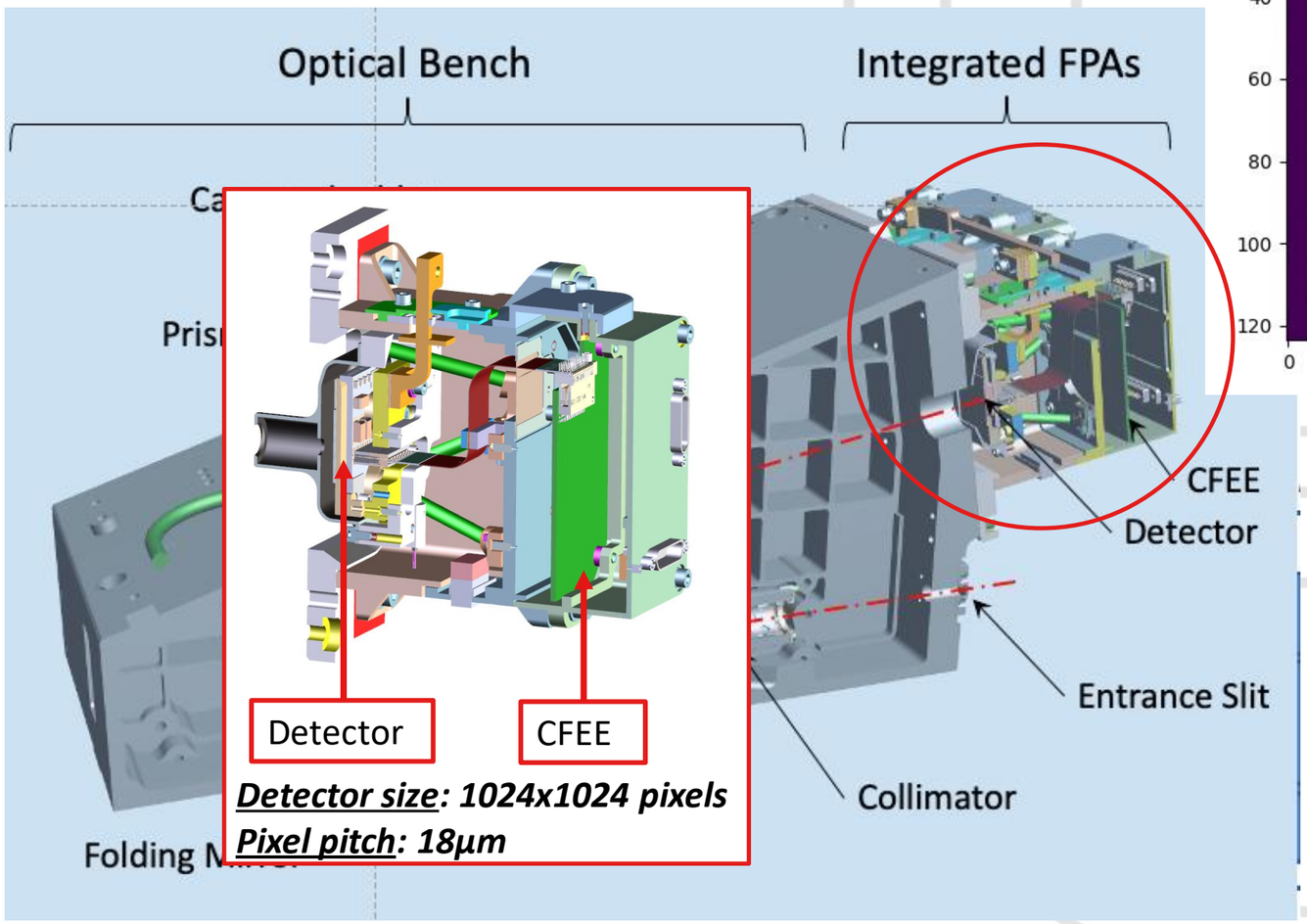

AIRS instrument : Optics Unit

- Minimum SIDECAR operating temperature is incompatible with ARIEL architecture.
  - → **No SIDECAR electronic is used (close to the detector)**
  - → **We had to design the Detector Control Unit**
- Observational strategy requires extremely good detector stability (up to 10 hours)
  - → **The acquisition chain is designed to be very stable**

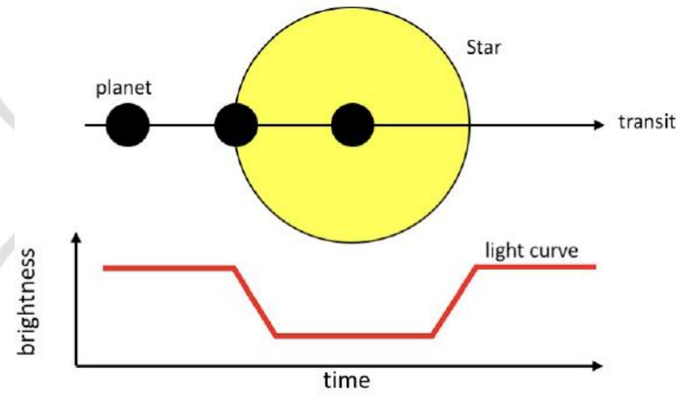

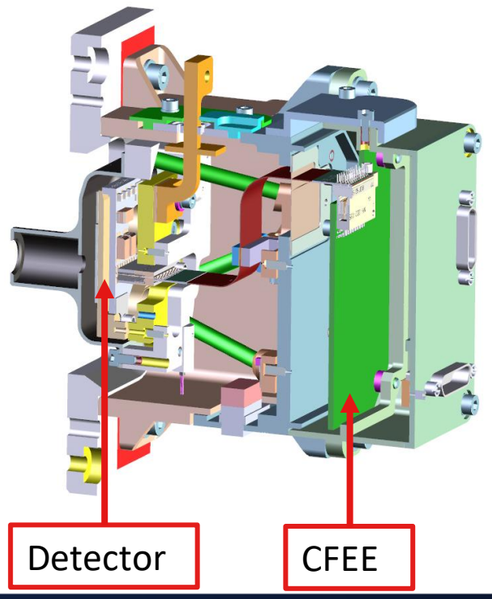

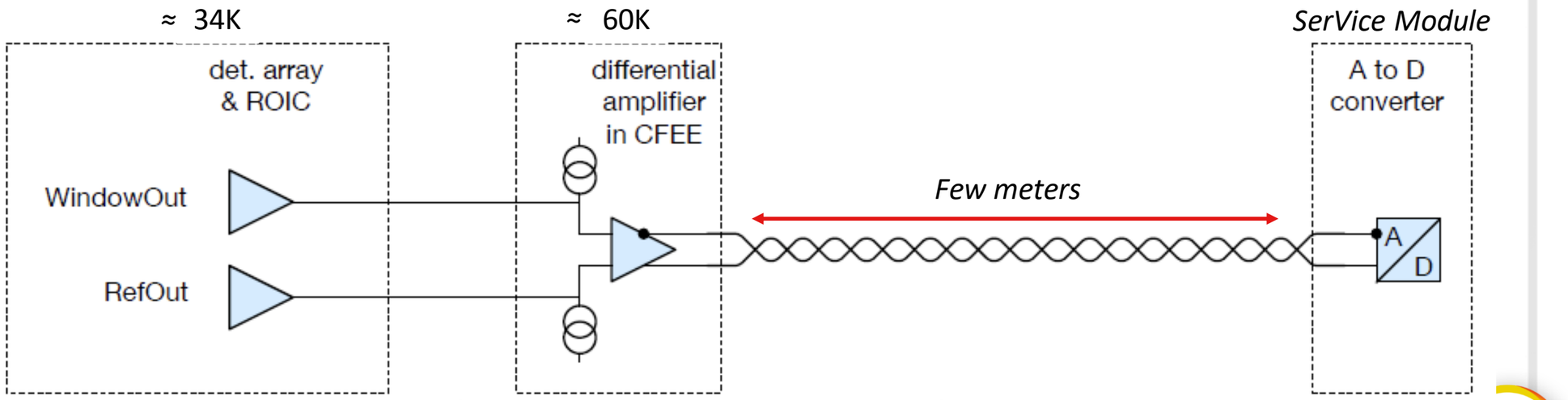

Schematic view of the AIRS acquisition chain

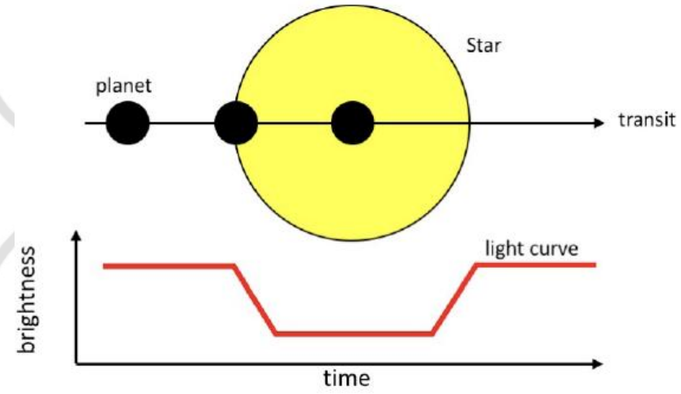

- Minimum SIDECAR operating temperature is incompatible with ARIEL architecture.
  - → **No SIDECAR electronic is used (close to the detector)**
  - → **We had to design the Detector Control Unit**
- Observational strategy requires extremely good detector stability (up to 10 hours)
  - → **The acquisition chain is designed to be very stable**
- General detector operation:
  - Operated in window mode: **355x64 for CH0, 130x64 for CH1**
  - Readout rate 100kpixel/s
  - AIRS acquisition chain operates in fully differential mode ➔ to suppress common-mode noise
  - **Separate reference output** permanently connected to V_{reset} , completely independent output

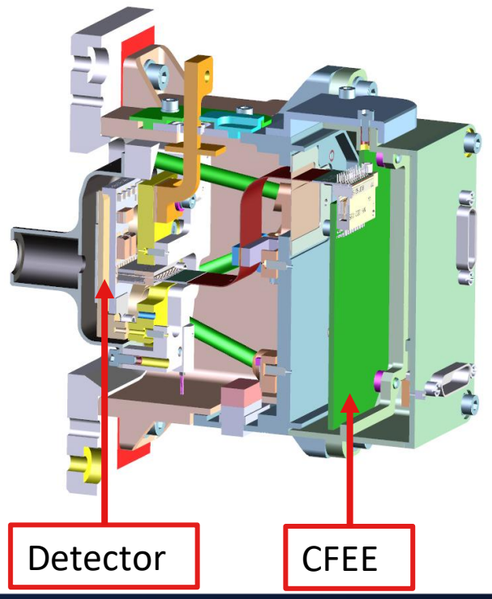

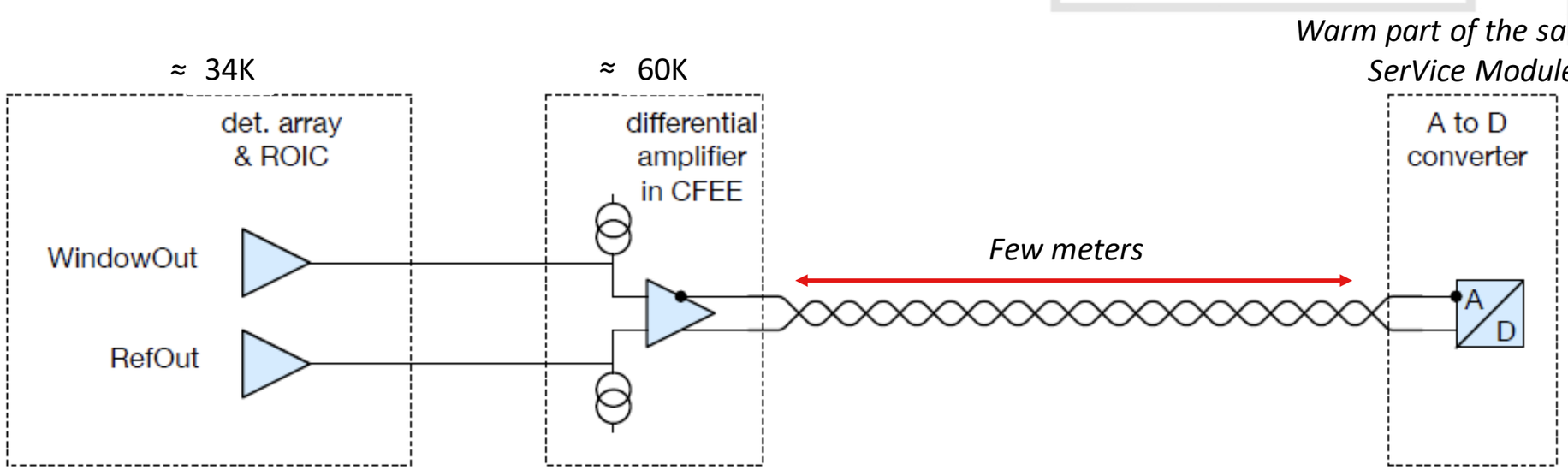

Schematic view of the AIRS acquisition chain

- Minimum SIDECAR operating temperature is incompatible with ARIEL architecture.
  - → **No SIDECAR electronic is used (close to the detector)**
  - → **We had to design the Detector Control Unit**

- Observational strategy requires extremely good detector stability (up to 10 hours)
  - → **The acquisition chain is designed to be very stable**

- General detector c
  - Operated ir
  - Readout ra
  - AIRS acquis
  - **Separate re**

de noise
t output

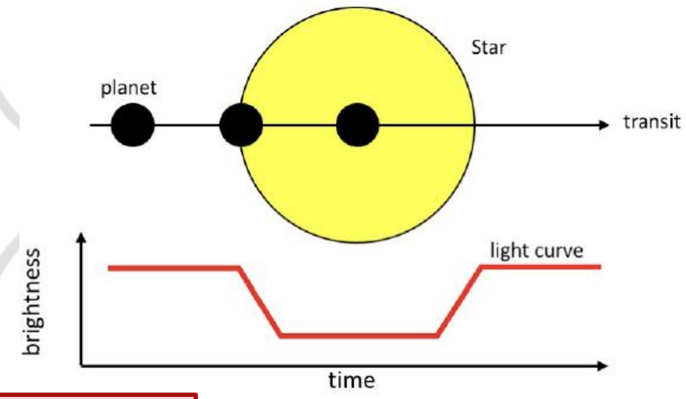

Need to characterize and calibrate the detectors to determine its behavior

To disantangle astrophysical effects from detector effects

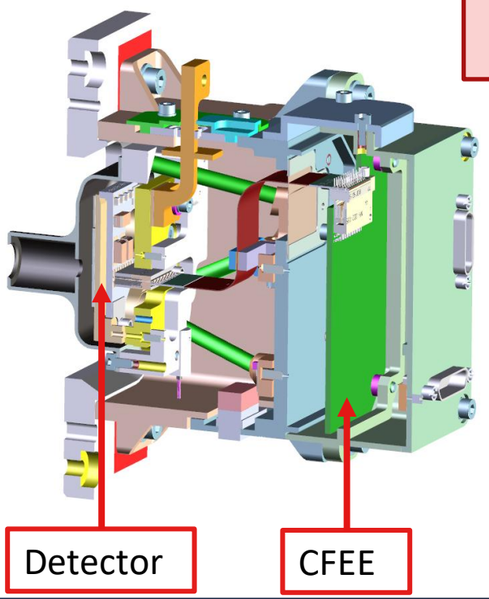

Warm part of the satellite, SerVice Module

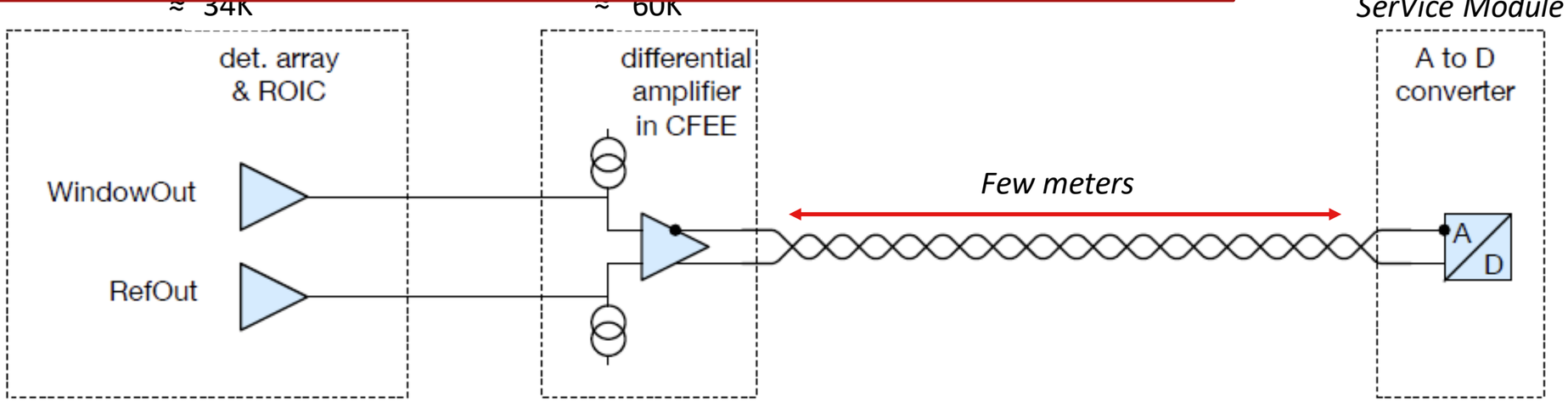

Schematic view of the AIRS acquisition chain

Plan

1. AIRS: ARIEL Infrared Spectrometer
    1. ARIEL space mission
    2. ARIEL spacecraft
    3. AIRS Acquisition chain architecture
2. Test bench at CEA
    1. Test bench presentation
3. Detector characterization results
    1. Strategy of calibration
    2. Detector baseline
    3. CDS and readout noise
    4. Dark current
    5. Readout glow
    6. Crosstalk
    7. Conversion gain and stability
4. Conclusion & Perspectives

2. Test bench at CEA
1. Test bench presentation

Test facilities in a cleanroom to characterize detectors

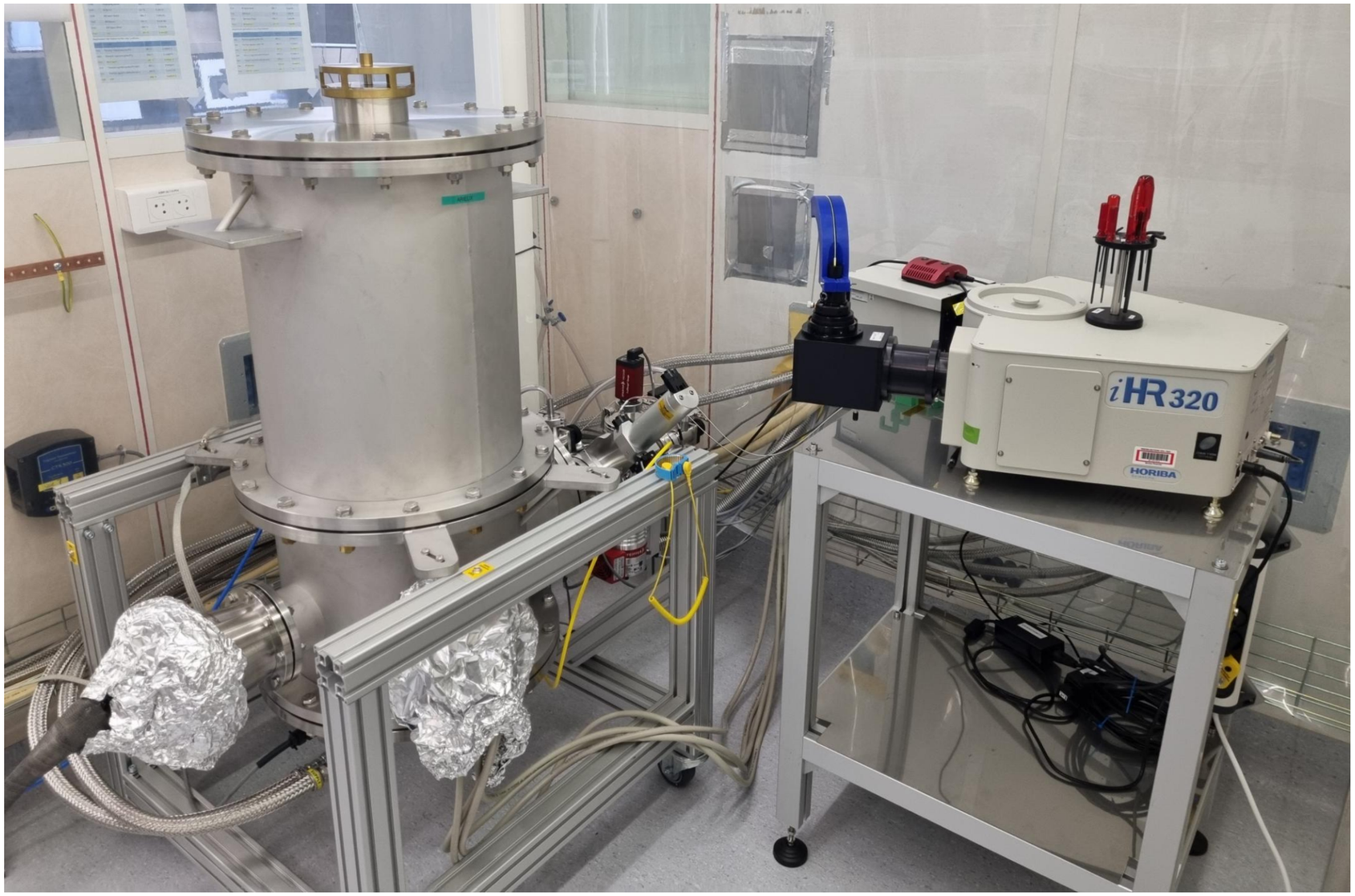

Picture of the test bench at CEA

Temperature ranges :
Detector : [32-42K]
CFEE : [55K-65K]
ADCU : 300K

Thermal control of the detector within ±5 mK for several hours.

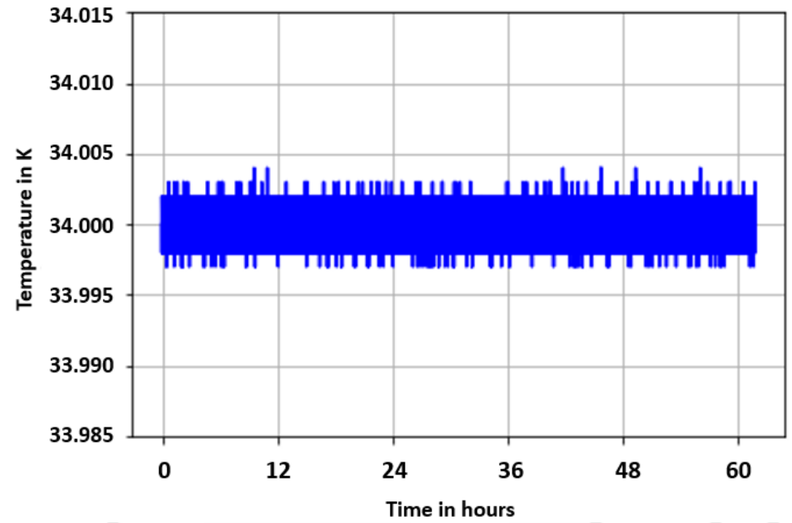

Detector temperature over 60 hours

Fine thermal stabilisation provided by the DCU

2. Test mean at CEA
1. Presentation of the test bench

Cold front end electronics

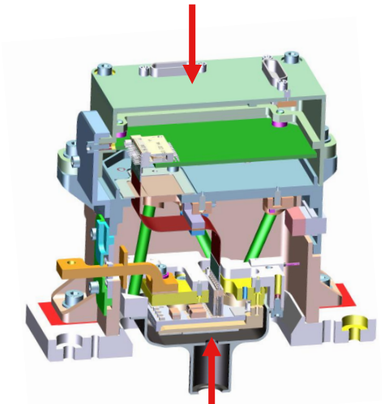

Detector (Teledyne H1RG detector)

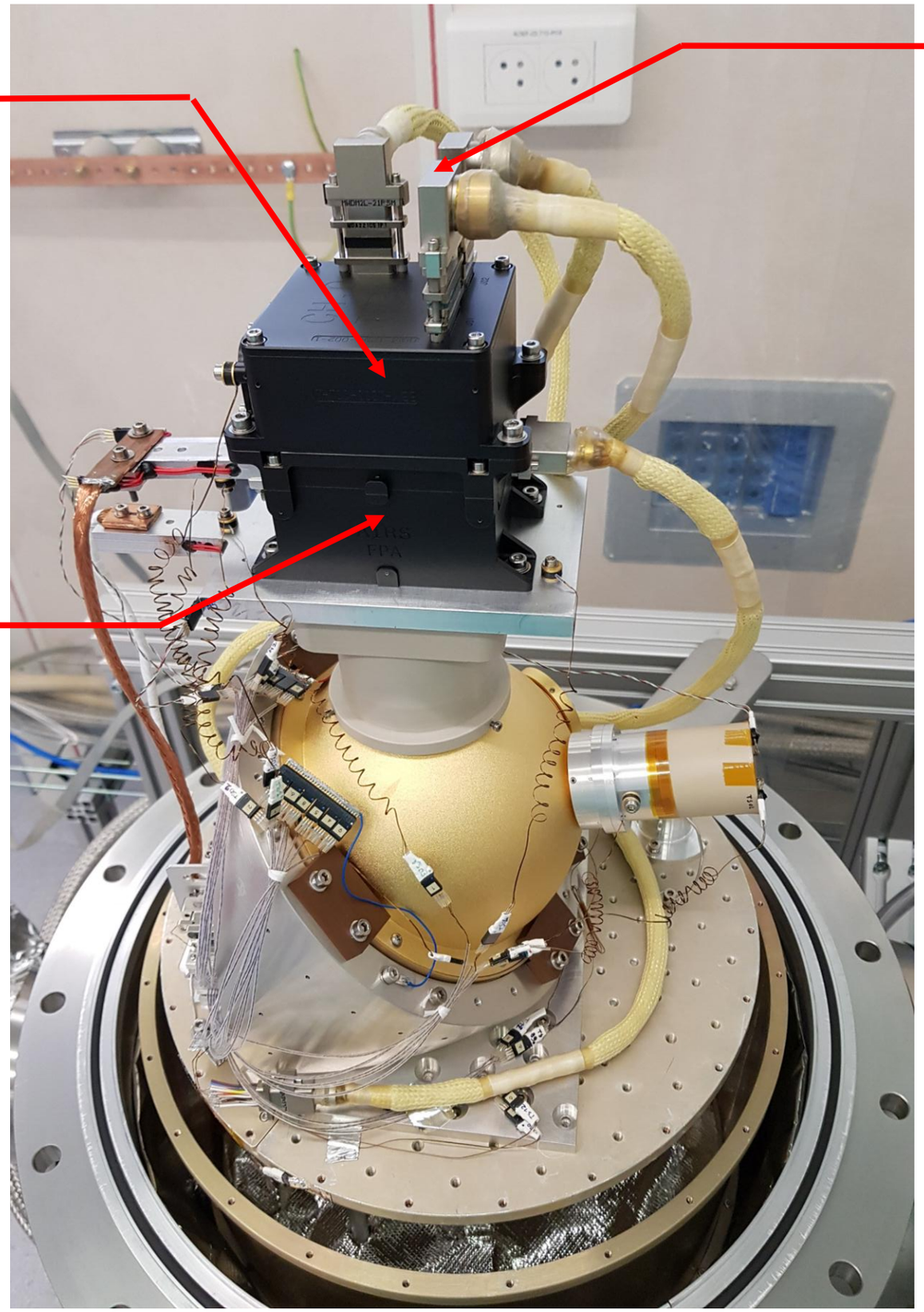

	EM CH0	EM CH1
Pixel array	1024x1024	1024x1024
Pixel pitch	18 µm	18 µm
Window size	355x64	130x64
λ_c (@ 32K)	4.75 µm	8.09 µm
Readout circuit	SFD (Source Follower Detector)	

Non-destructive readout

2. Test mean at CEA
1. Presentation of the test bench

Cold front end electronics

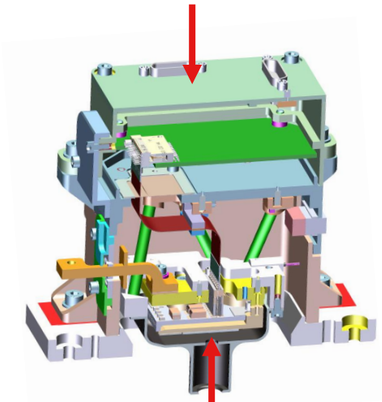

Detector (Teledyne H1RG detector)

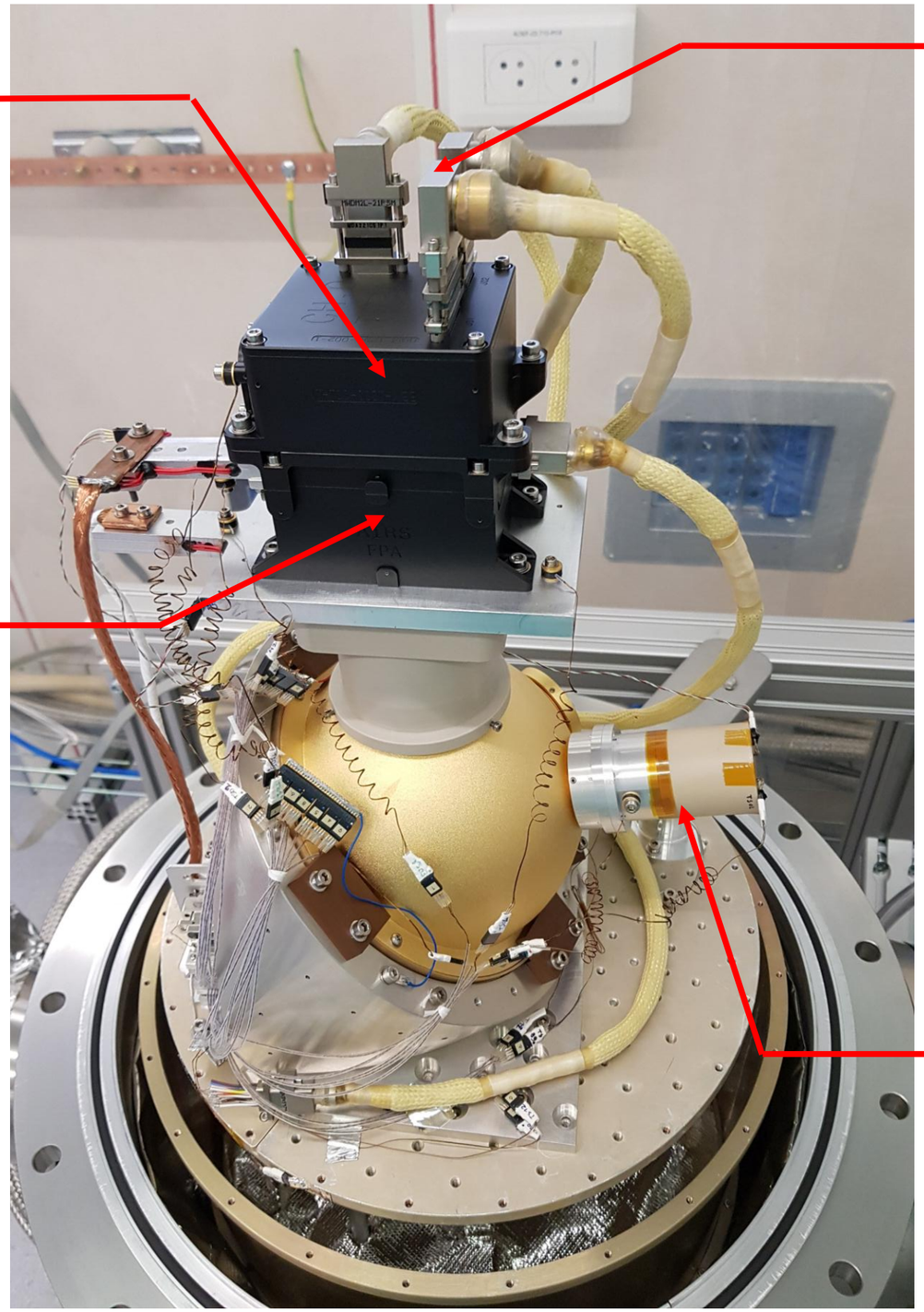

Connecting Harnesses

Cryogenic black body

- A filter can be placed in front of the blackbody (transmission characteristic was measured at low temperature at ESA)

	EM CH0	EM CH1
Pixel array	1024x1024	1024x1024
Pixel pitch	18 µm	18 µm
Window size	355x64	130x64
λ_c (@ 32K)	4.75 µm	8.09 µm
Readout circuit	SFD (Source Follower Detector)	

Non-destructive readout

2. Test mean at CEA
1. Presentation of the test bench

Cold front end electronics

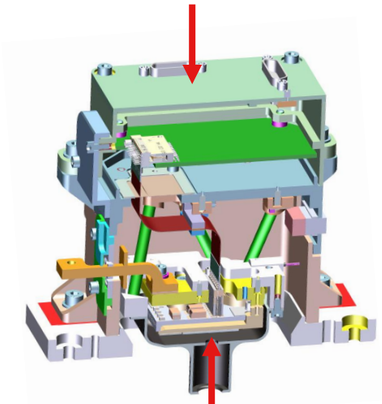

Detector (Teledyne H1RG detector)

	EM CH0	EM CH1
Pixel array	1024x1024	1024x1024
Pixel pitch	18 µm	18 µm
Window size	355x64	130x64
λ_c (@ 32K)	4.75 µm	8.09 µm
Readout circuit	SFD (Source Follower Detector)	

Non-destructive readout

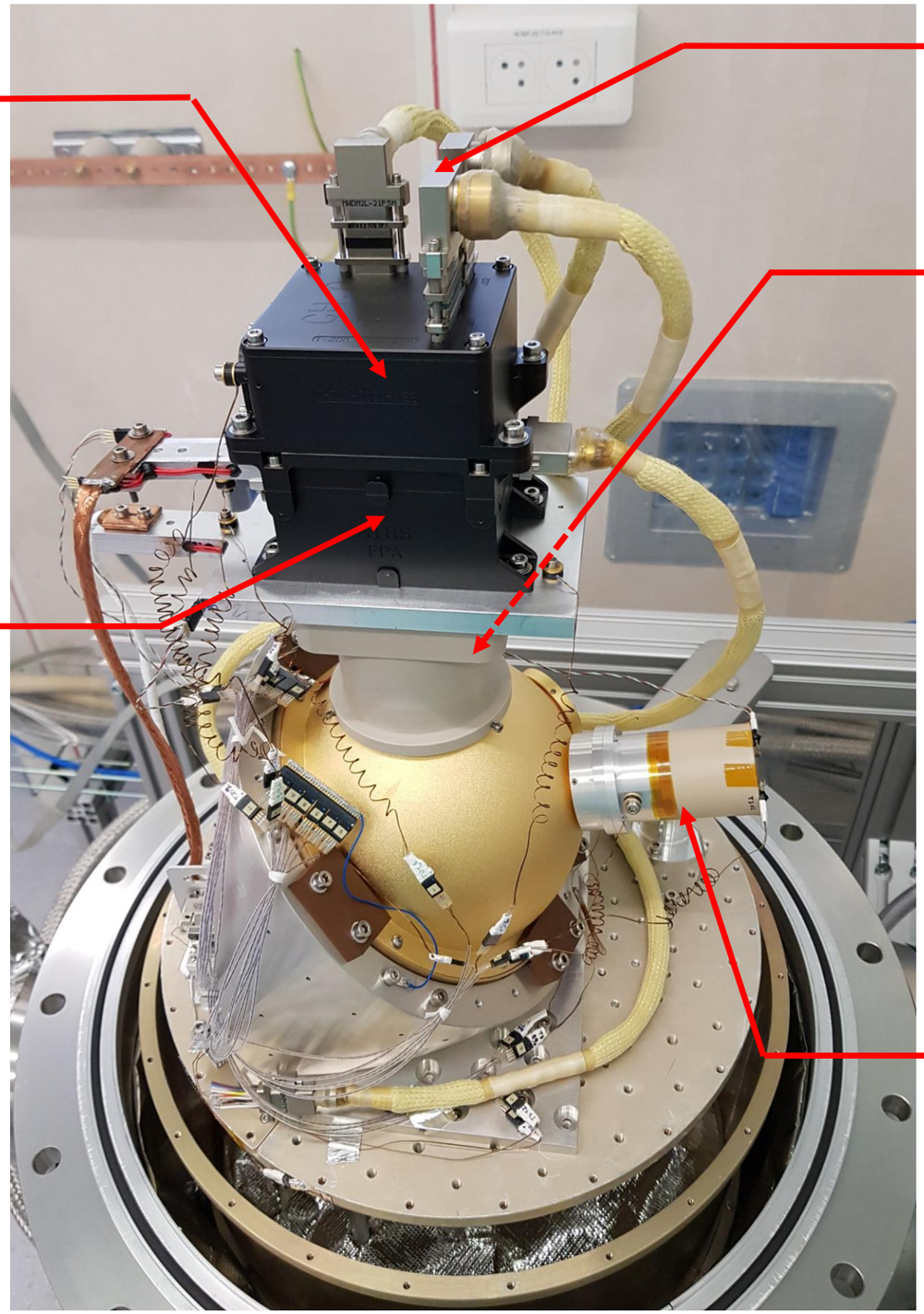

Connecting Harnesses

Available port for a photodiode

- Photodiode to know the incident flux on the detector

Cryogenic black body

- A filter can be placed in front of the blackbody (transmission characteristic was measured at low temperature at ESA)

2. Test mean at CEA
1. Presentation of the test bench

Cold front end electronics

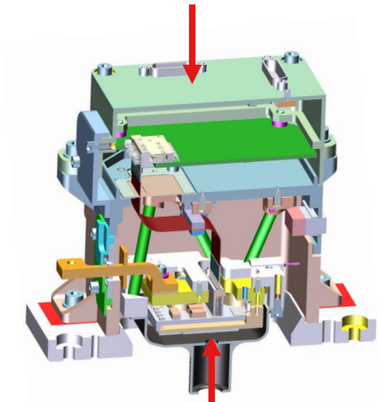

Detector (Teledyne H1RG detector)

	EM CH0	EM CH1
Pixel array	1024x1024	1024x1024
Pixel pitch	18 µm	18 µm
Window size	355x64	130x64
λ_c (@ 32K)	4.75 µm	8.09 µm
Readout circuit	SFD (Source Follower Detector)	

Non-destructive readout

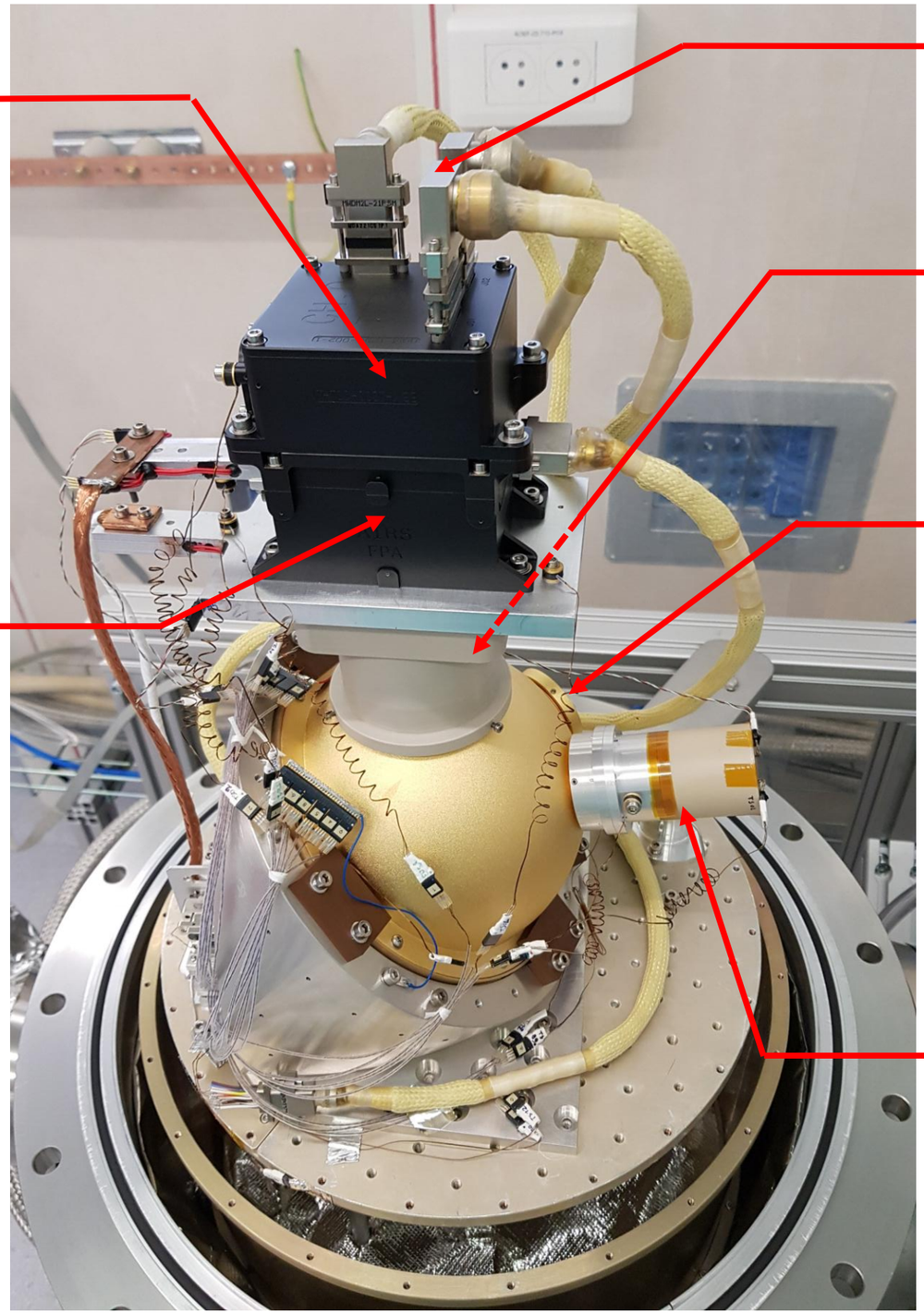

Connecting Harnesses

Available port for a photodiode

- Photodiode to know the incident flux on the detector

Available port for a LED or optical fiber

- LED at 3.4 µm for persistence measurement
- 2 optical fibers for CH0 and CH1 detectors (QE spectral measurement)

Cryogenic black body

- A filter can be placed in front of the blackbody (transmission characteristic was measured at low temperature at ESA)

2. Test mean at CEA
1. Presentation of the test bench

Cold front end electronics

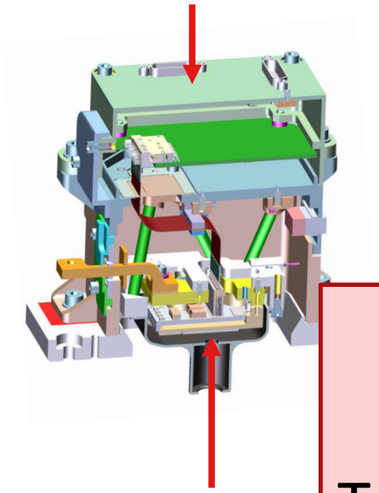

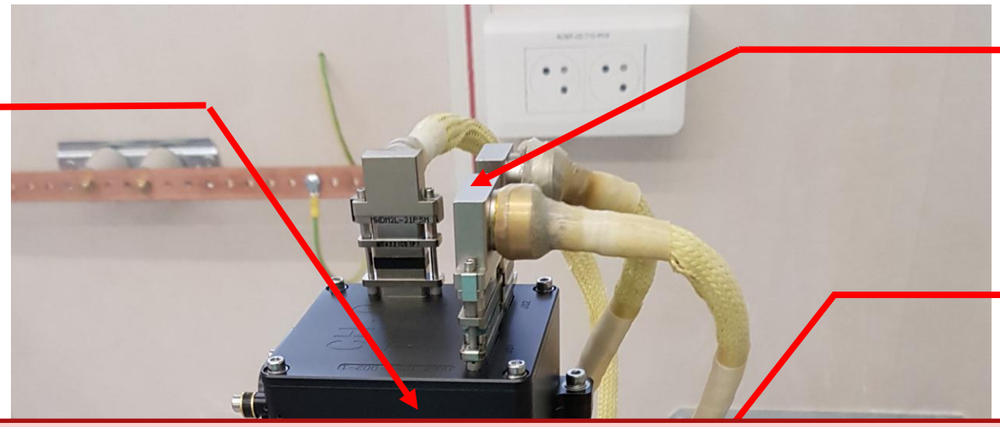

Connecting Harnesses

Available port for a photodiode
- Photodiode to know the incident flux on the detector

Detector (Teledyne H1RG

Test bench ➔ to realize several measurements for the characterization of detectors

port for a LED or optical

.4 µm for persistence
ement
l fibers for CH0 and CH1
rs (QE spectral measurement)

	EM CH0	
Pixel array	1024x1024	
Pixel pitch	18 µm	18 µm
Window size	355x64	130x64
λ_c (@ 32K)	4.75 µm	8.09 µm
Readout circuit	SFD (Source Follower Detector)	

Non-destructive readout

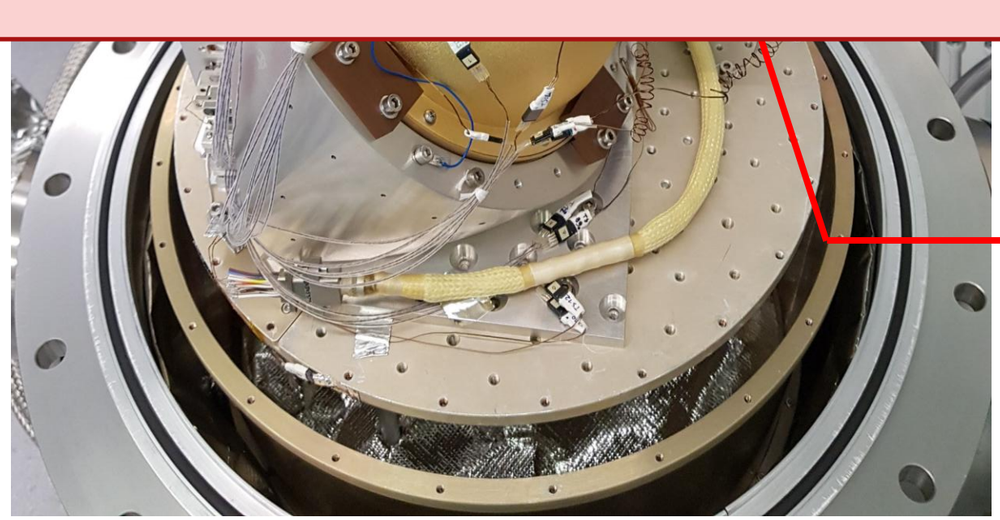

Cryogenic black body
- A filter can be placed in front of the blackbody (transmission characteristic was measured at low temperature at ESA)

Plan

1. AIRS: ARIEL Infrared Spectrometer
    1. ARIEL space mission
    2. ARIEL spacecraft
    3. AIRS Acquisition chain architecture
2. Test bench at CEA
    1. Test bench presentation
3. Detector characterization results
    1. Strategy of calibration
    2. Detector baseline
    3. CDS and readout noise
    4. Dark current
    5. Readout glow
    6. Crosstalk
    7. Conversion gain and stability
4. Conclusion & Perspectives

EM CH0 and CH1 detectors

Strategy of Engineering/Flight Model calibration :

- ❑ Verification of environment's thermal stability after the cryostat closing
- ❑ Testing implementation for optimization of operating point + validation
- ❑ Calibration of the detector and Cold Front End Electronics (only, no optical elements)

To take into account mechanical and optical margins:

CH0 detector : Illustration of windows considered throughout the calibration

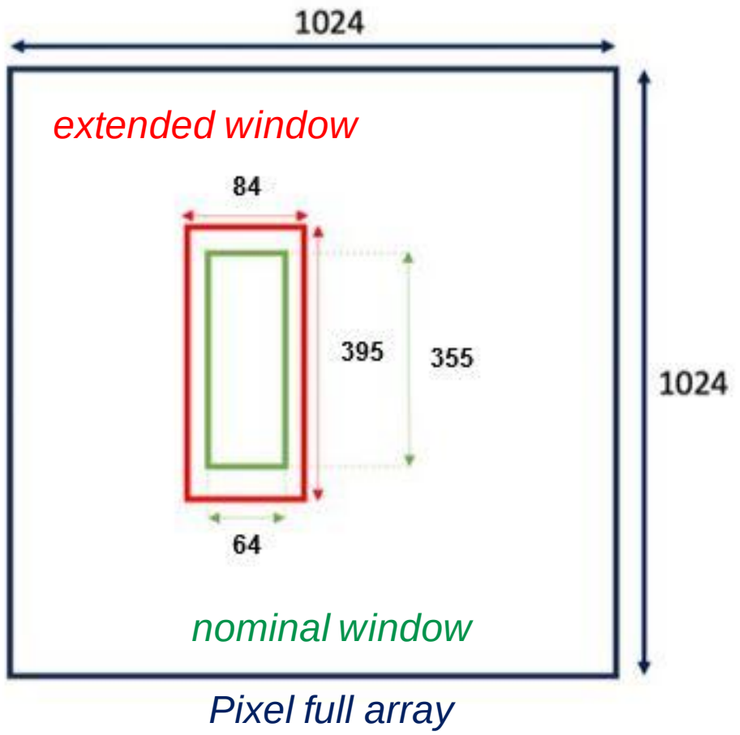

	CH0	CH1
Nominal window size	355x64	130x64
Extended window size	395x84	170x84

EM CH0 and CH1 detectors

Strategy of Engineering/Flight Model calibration :

- ❑ Verification of environment's thermal stability after the cryostat closing
- ❑ Testing implementation for optimization of operating point + validation
- ❑ Calibration of the detector and Cold Front End Electronics (only, no optical elements)

To take into account mechanical and optical margins:

CH0 detector : Illustration of windows considered throughout the calibration

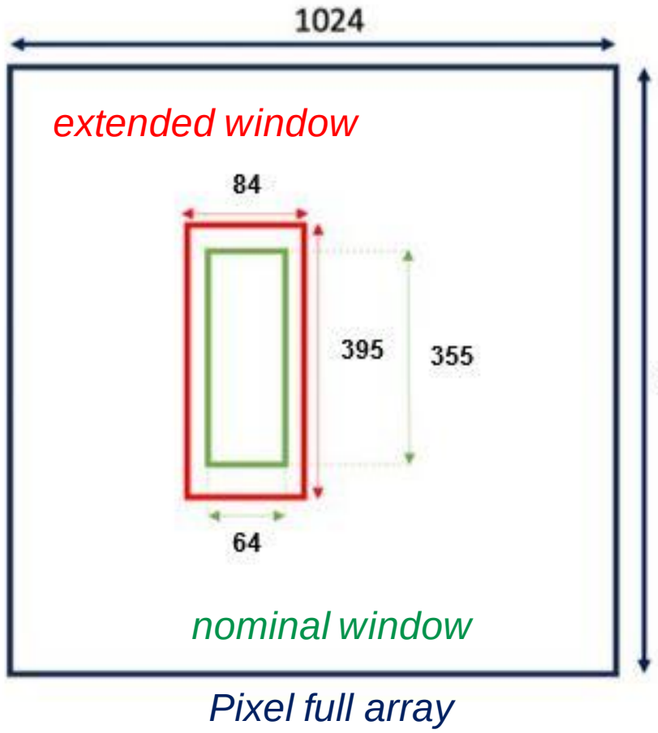

	CH0	CH1
Nominal window size	355x64	130x64
Extended window size	395x84	170x84

Schematic view of readout sequence (not at scale)

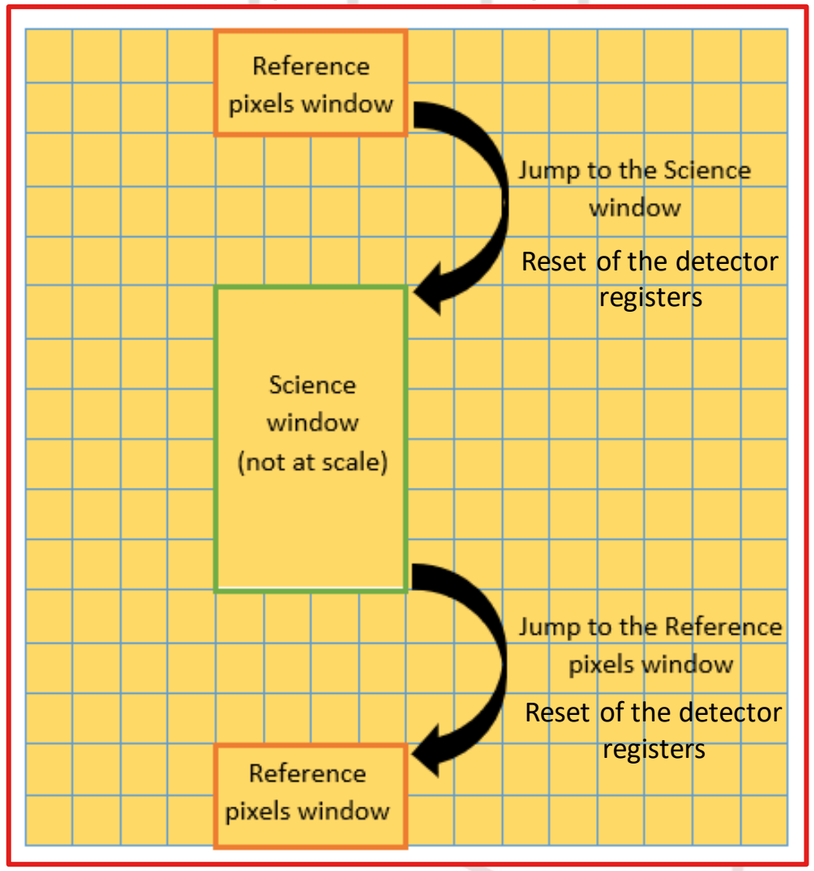

EM CH0 and CH1 detectors

Strategy of Engineering/Flight Model calibration :

- ❑ Verification of environment's thermal stability after the cryostat closing
- ❑ Testing implementation for optimization of operating point + validation
- ❑ Calibration of the detector and Cold Front End Electronics (only, no optical elements)

To take into account mechanical and optical margins:

CH0 detector : Illustration of windows considered throughout the calibration

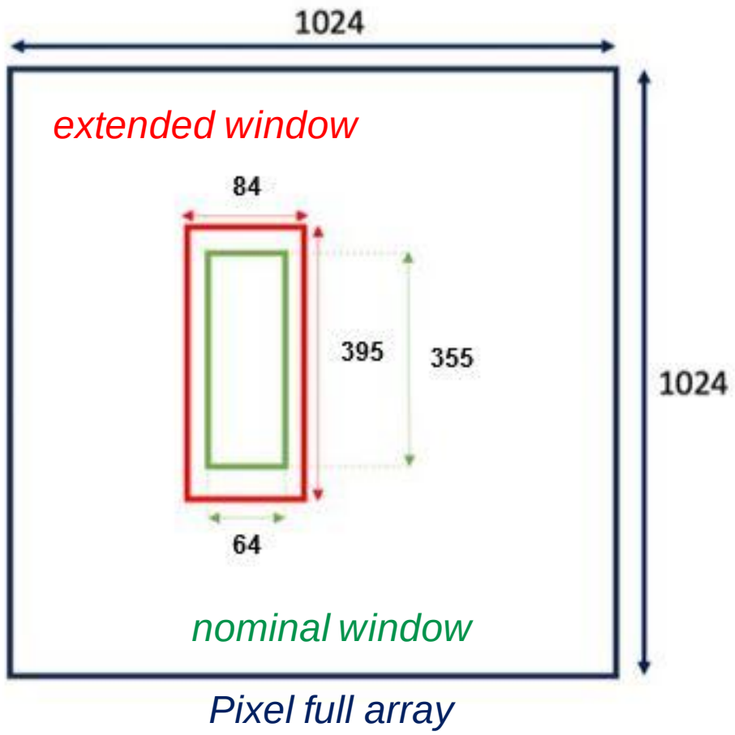

	CH0	CH1
Nominal window size	355x64	130x64
Extended window size	395x84	170x84

List of the calibration product as function of detector temperature (32K-42K)

ID	TITLE
R-ACAL-010	Ground Pixel Operability
R-ACAL-020	Ground calibration of Full Well Dynamics
R-ACAL-030	Ground Acquisition Chain Gain
R-ACAL-040	Non-Linearity
R-ACAL-060	Dark current
R-ACAL-070	Relative QE
R-ACAL-095	SuperBias
R-ACAL-100	Persistence
R-ACAL-120	Ground Read Out noise

EM CH0 and CH1 detectors

Strategy of Engineering/Flight Model calibration :

- ❑ Verification of environment's thermal stability after the cryostat closing
- ❑ Testing implementation for optimization of operating point + validation
- ❑ Calibration of the detector and Cold Front End Electronics (only, no optical elements)

Optimization of the operating point

Bias	EM CH0	EM CH1
VDD	3.3V	3.3V
VDDA	3.3V	3.3V
VBIASGATE	2.3V	2.285V
VBIASPOWER	3.3V	3.3V
DETECTOR BIAS	250mV	250mV
VRESET	150mV	250mV
CELLDRAIN	0V	0V

List of the calibration product as function of detector temperature (32K-42K)

ID	TITLE
R-ACAL-010	Ground Pixel Operability
R-ACAL-020	Ground calibration of Full Well Dynamics
R-ACAL-030	Ground Acquisition Chain Gain
R-ACAL-040	Non-Linearity
R-ACAL-060	Dark current
R-ACAL-070	Relative QE
R-ACAL-095	SuperBias
R-ACAL-100	Persistence
R-ACAL-120	Ground Read Out noise

Reference pixels (top)

Active pixels

Reference pixels (bottom)

Series of 400 images in 200 integrations

MWIR EM CH0

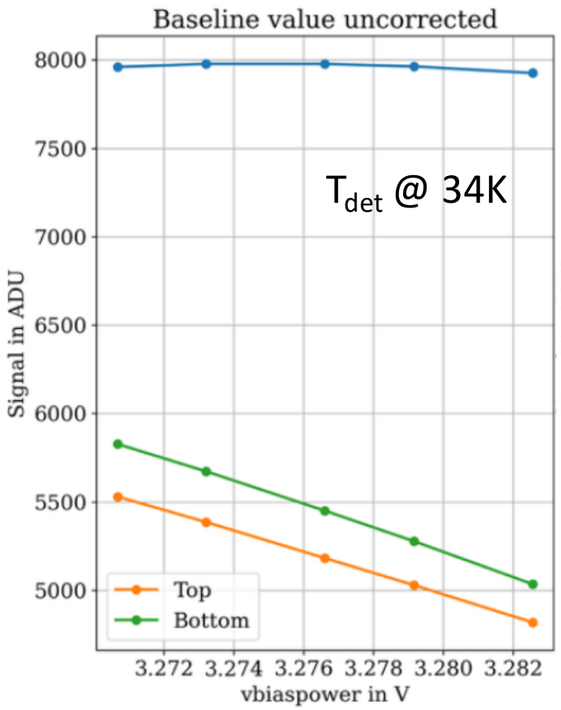

VBIASPOWER

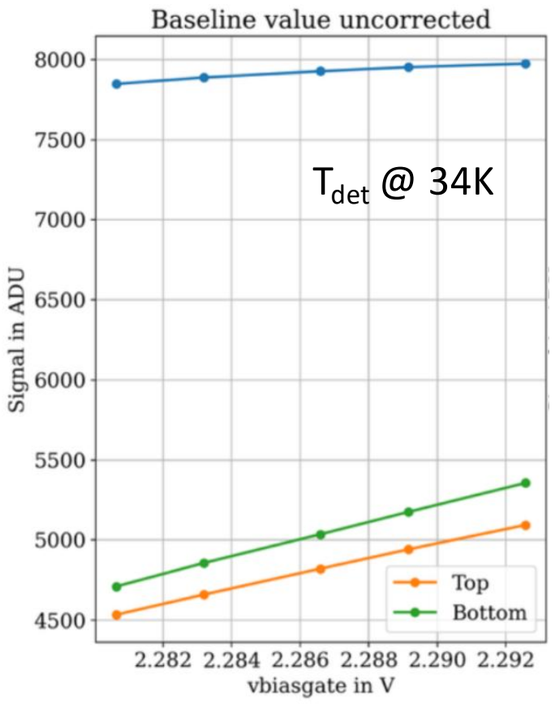

VBIASGATE

LWIR EM CH1

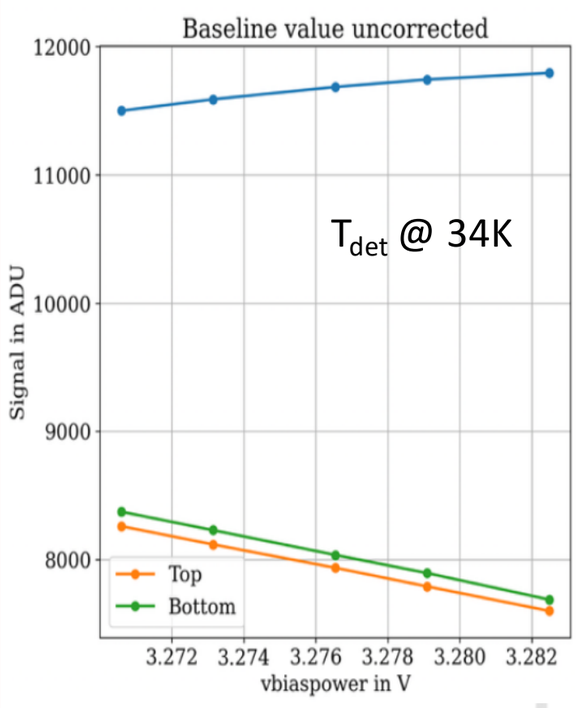

VBIASPOWER

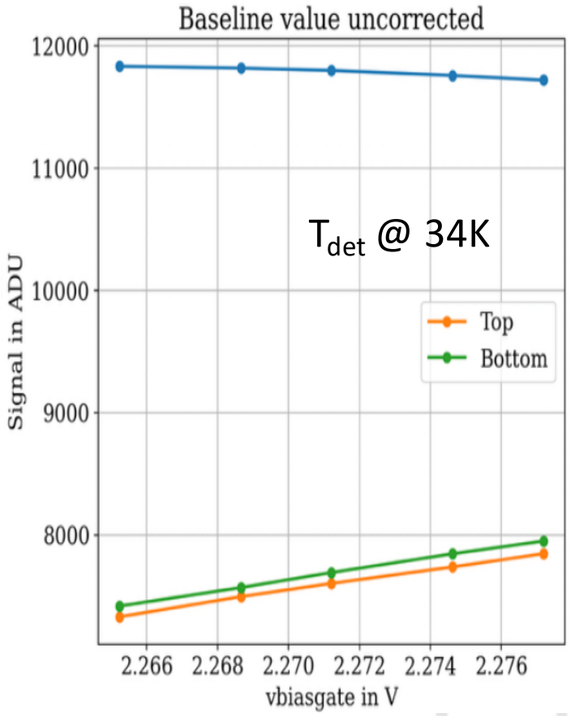

VBIASGATE

Reference pixels (top)

Active pixels

Reference pixels (bottom)

Series of 400 images in 200 integrations

MWIR EM CH0

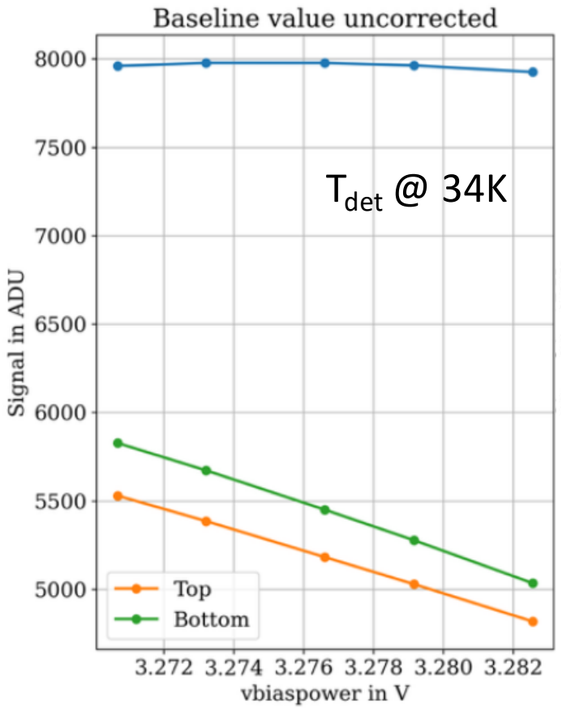

VBIASPOWER

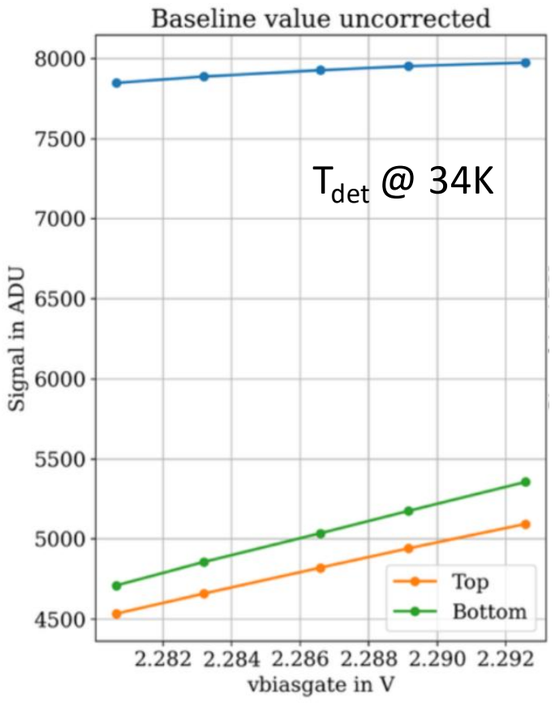

VBIASGATE

LWIR EM CH1

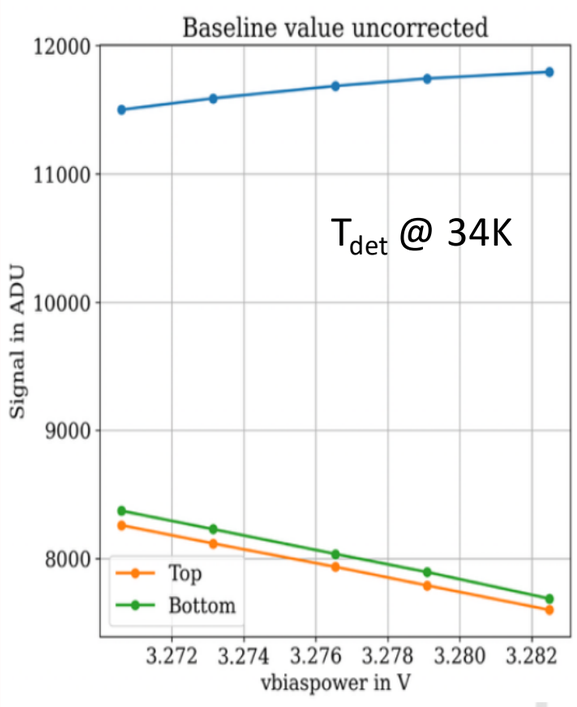

VBIASPOWER

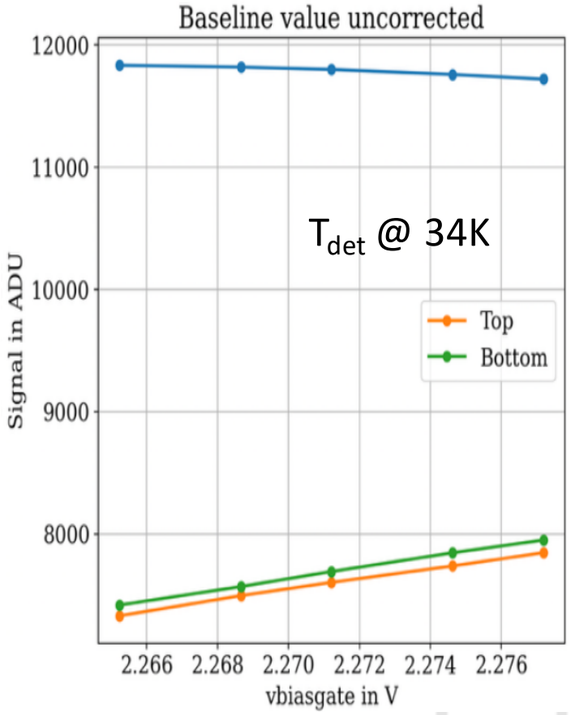

VBIASGATE

Difference in evolution of the baseline as function of biases for active pixels and reference pixels

Variations more important for reference pixels

Unexpected results, investigation on going

Series of 180 CDS images

- CDS images calculated
- Standard deviation computed for each pixel

CDS noise		
	CH0	**CH1**
	MWIR	**LWIR**
Median	**13.25**	**13.37**
5%	**12.22**	**12.47**
95%	**17.33**	**18.16**

Results in e⁻

MWIR EM CH0

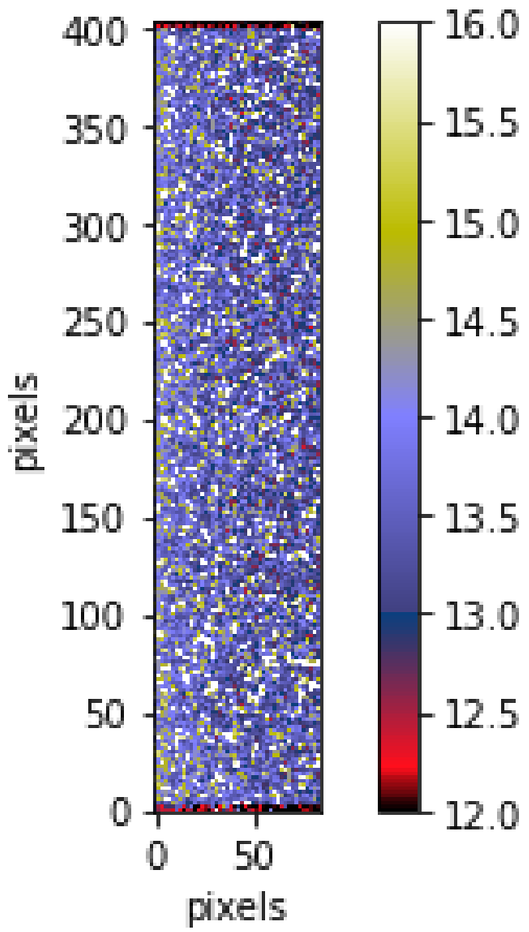

LWIR EM CH1

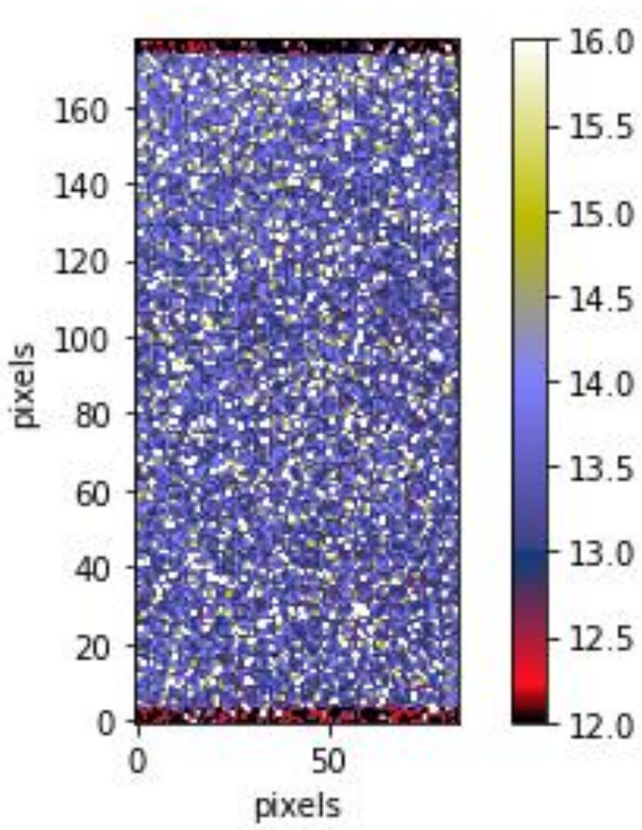

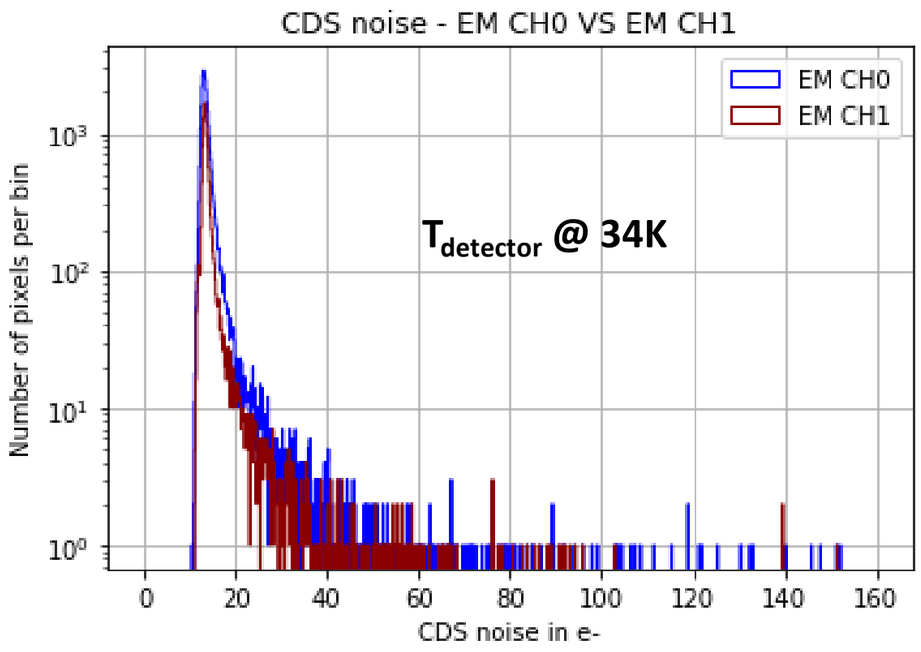

Median gain conversion : **2.22 e⁻/ADU** (CH0) and **2.18 e⁻/ADU** (CH1)

Series of 180 CDS images

- CDS images calculated
- Standard deviation computed for each pixel

CDS noise		
	CH0	**CH1**
	MWIR	**LWIR**
Median	**13.25**	**13.37**
5%	**12.22**	**12.47**
95%	**17.33**	**18.16**

Results in e⁻

MWIR EM CH0

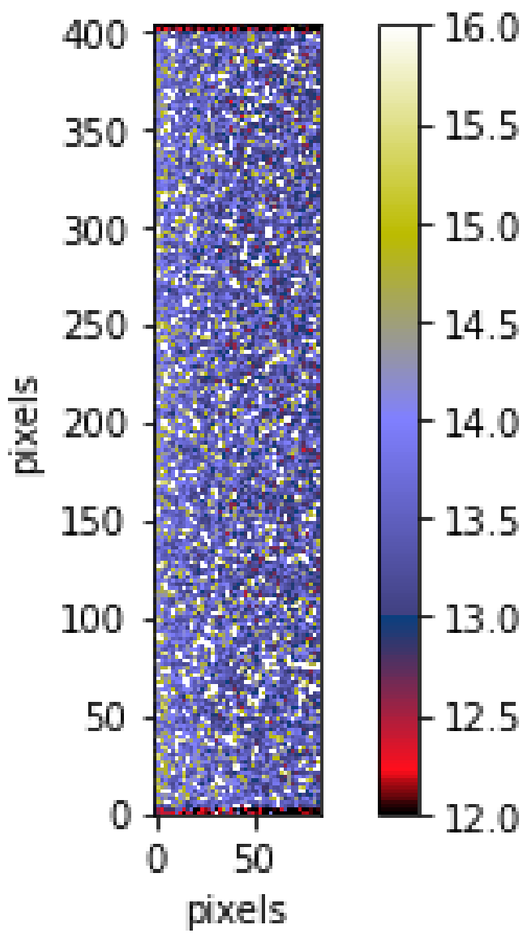

LWIR EM CH1

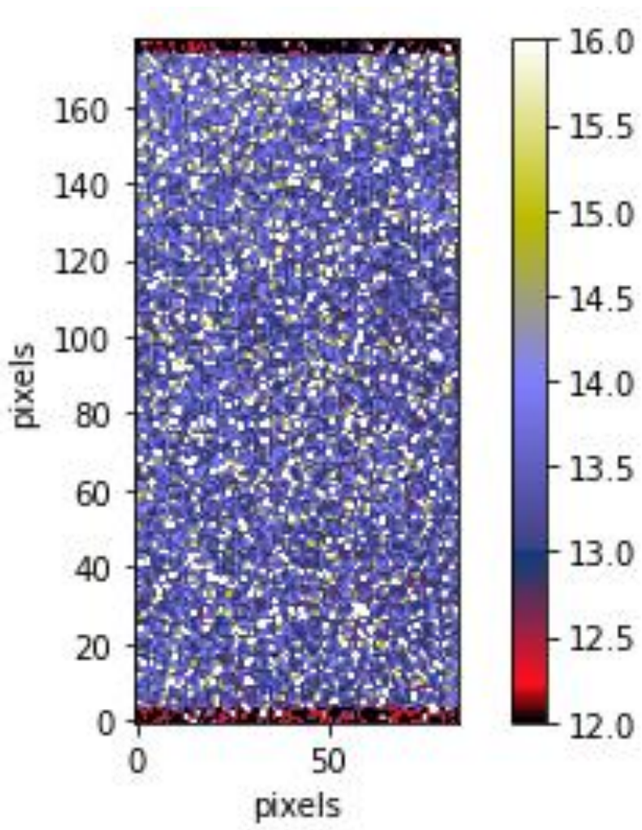

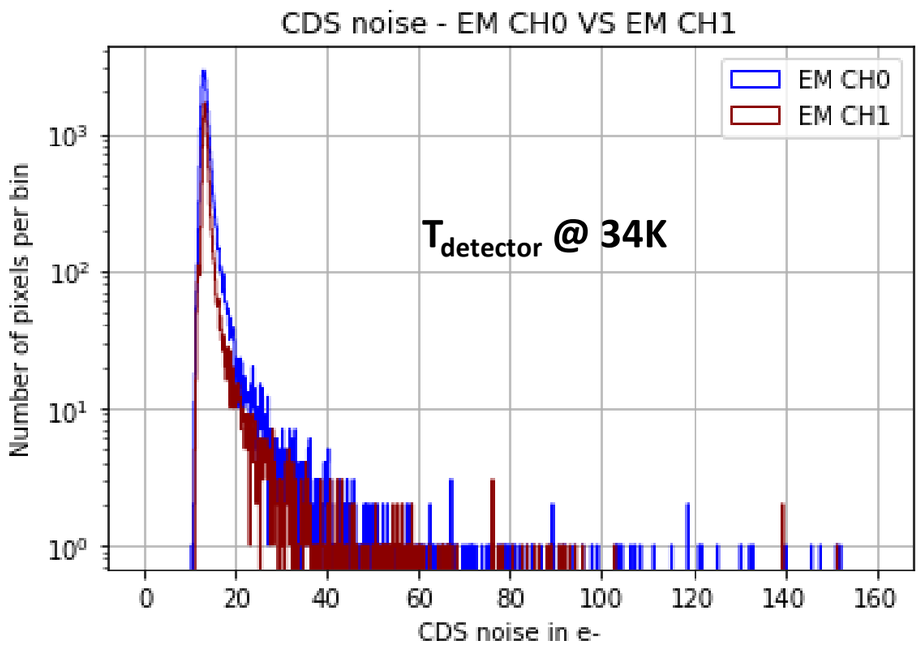

Median gain conversion : **2.22 e⁻/ADU** (CH0) and **2.18 e⁻/ADU** (CH1)

Compliant with AIRS specifications

Median gain conversion : **2.22 e⁻/ADU** (CH0) and **2.18 e⁻/ADU** (CH1)

Dark current measurements : **5 hours**

MWIR EM CH0

4 series of 10851 images

Linear regression fit

Median dark current

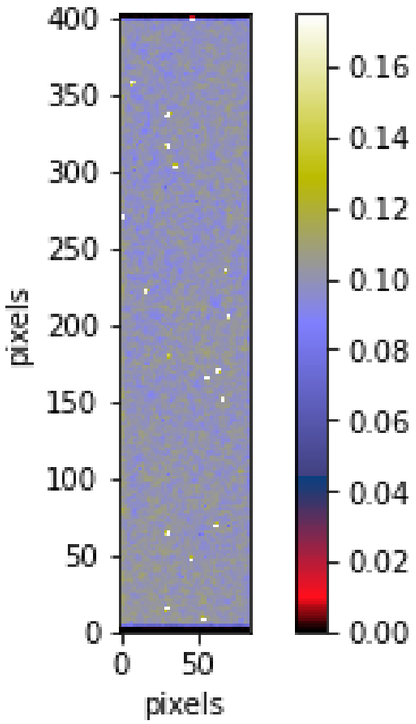

Number of outliers (>5σ) = **58** **(0.2%)**

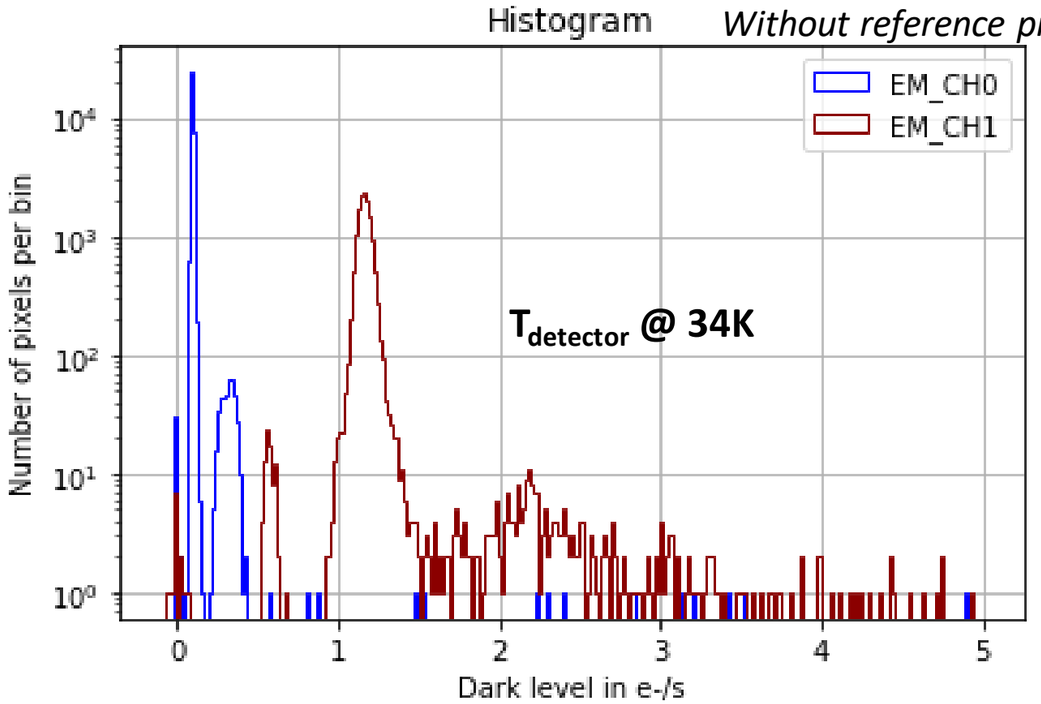

in e⁻/s/pix	EM CH0	EM CH1
Mean	0.104	1.195
Median	0.10	1.166
Min	-0.010	-0.104
Max	5.177	10.361
5%	0.090	1.099
25%	0.096	1.138
75%	0.104	1.195
95%	0.111	1.259

LWIR EM CH1

4 series of 22372 images

Linear regression fit

Median dark current

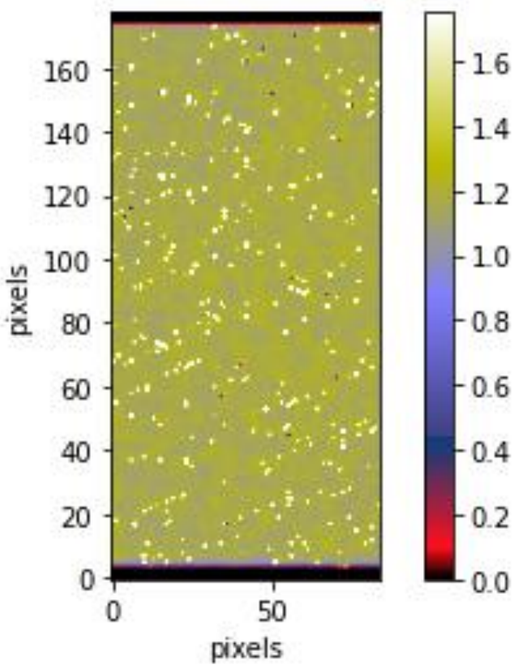

Number of outliers (>5σ) = **321** **(2.2%)**

Dark current measurements : **5 hours**

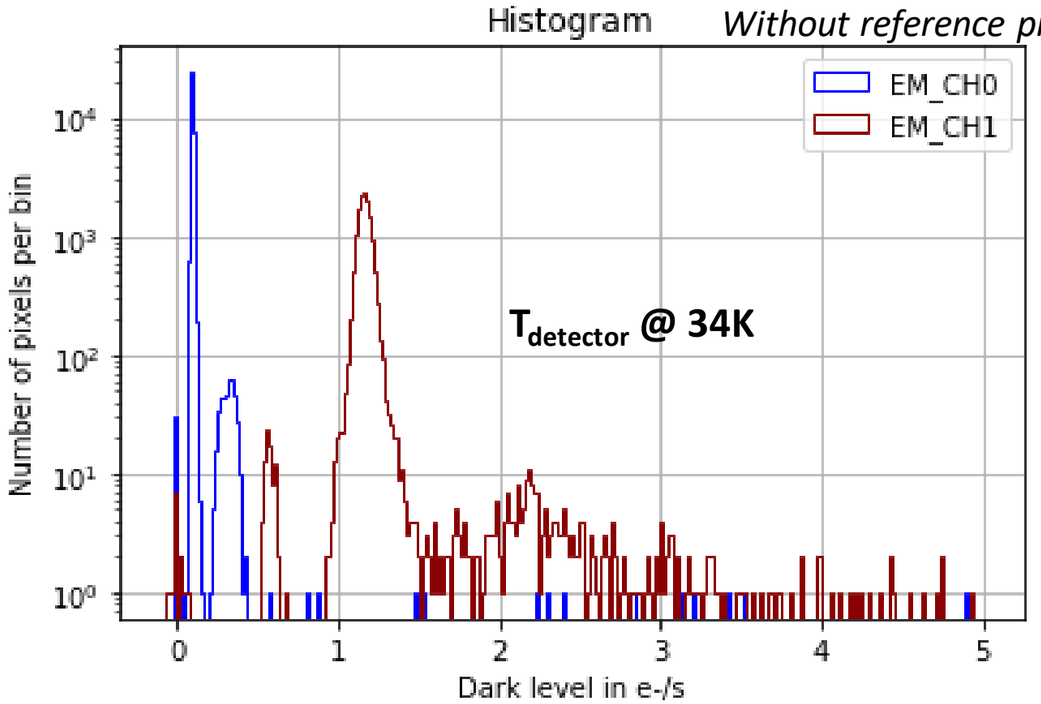

MWIR EM CH0

4 series of 10851 images

Linear regression fit

Median dark current

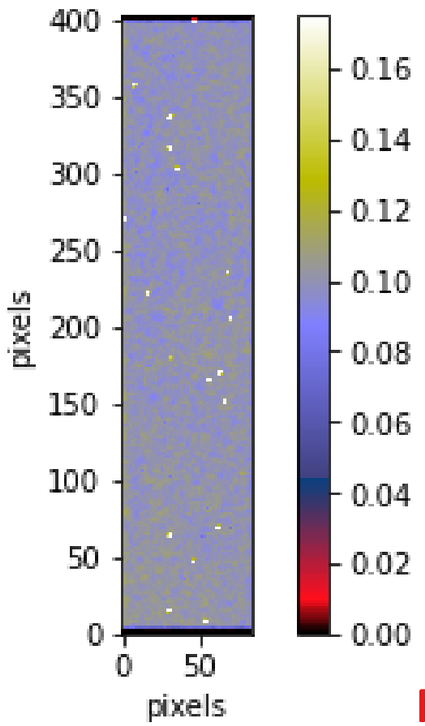

Number of outliers (>5σ) = **58** **(0.2%)**

in e⁻/s/pix	EM CH0	EM CH1
Mean	0.104	1.195
Median	0.10	1.166
Min	-0.010	-0.104
Max	5.177	10.361
5%	0.090	1.099
25%	0.096	1.138
75%	0.104	1.195
95%	0.111	1.259

LWIR EM CH1

4 series of 22372 images

Linear regression fit

Median dark current

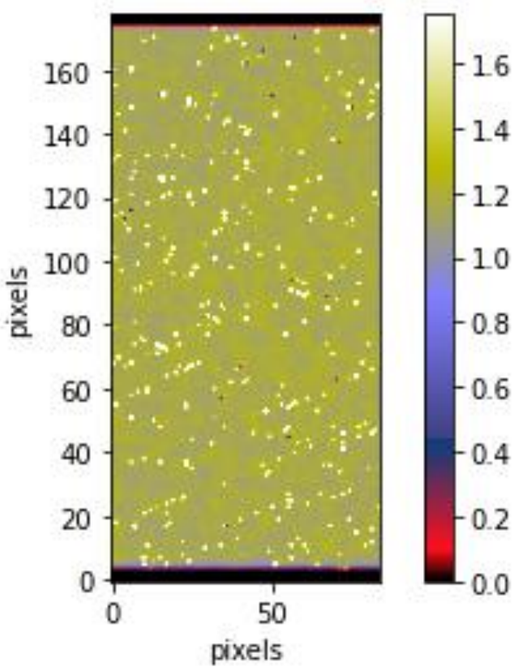

Number of outliers (>5σ) = **321** **(2.2%)**

No Compliant to AIRS requirements, but compliant to science needs

3. Characterization results
4. Dark current

Median gain conversion : **2.22 e⁻/ADU** (CH0) and **2.18 e⁻/ADU** (CH1)

- Detector baseline
- CDS and readout noise
- Dark current
- Readout glow
- Crosstalk
- Conversion gain

Dark current measurements : **5 hours**

MWIR EM CH0

LWIR EM CH1

Contribution of the pixel source follower **GLOW** in dark current measurements

MWIR EM CH0 Detector

$T_{detector}$ @ 34K

	Measurement	T_{det}	Light source	Readout mode	Line	Col	Frame time	Measurement duration	t_{int}	N_{ramps}	N_{groups}
1.0	Glow t_f	T_1	None	FUR	355	64	**0.227**	1800	1800	1	7920
1.1	Glow t_f + 1.0	T_1	None	FUR	355	64	**1.227**	1800	1800	1	1467
1.2	Glow t_f + 2.0	T_1	None	FUR	355	64	**2.227**	1800	1800	1	808

$$S_{Dark} = I_{Dark} + \frac{F}{dt} \quad (2)$$

Effective dark current

Real dark current

Glow per frame

Frame time

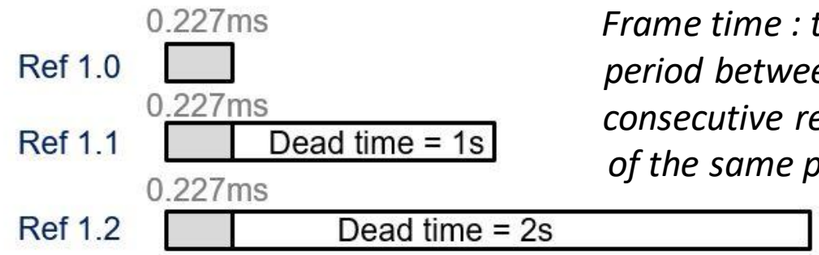

Frame time : time period between 2 consecutive reads of the same pixel

The global frame time is higher, the dark current is lower

(2) M. W. Regan, L. E. Bergeron, "Zero dark current in H2RG detectors: it is all multiplexer glow", J. Astron. Telesc. Instrum. Syst. 6(1), 016001 (2020)

MWIR EM CH0 Detector

$T_{detector}$ @ 34K

	Measurement	T_{det}	Light source	Readout mode	Line	Col	Frame time	Measurement duration	t_{int}	N_{ramps}	N_{groups}
1.0	Glow t_f	T_1	None	FUR	355	64	**0.227**	1800	1800	1	7920
1.1	Glow t_f + 1.0	T_1	None	FUR	355	64	**1.227**	1800	1800	1	1467
1.2	Glow t_f + 2.0	T_1	None	FUR	355	64	**2.227**	1800	1800	1	808

$$S_{Dark} = I_{Dark} + \frac{F}{dt} \quad (2)$$

Effective dark current

Real dark current

Glow per frame

Frame time

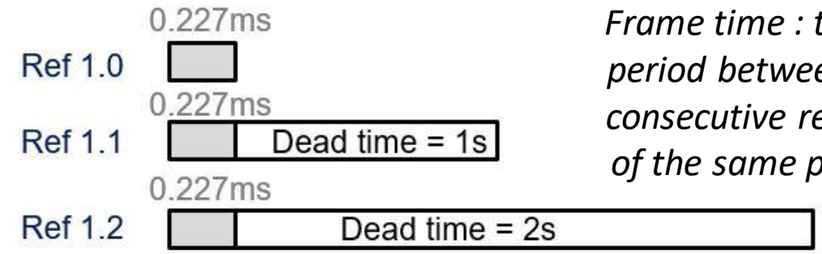

Frame time : time period between 2 consecutive reads of the same pixel

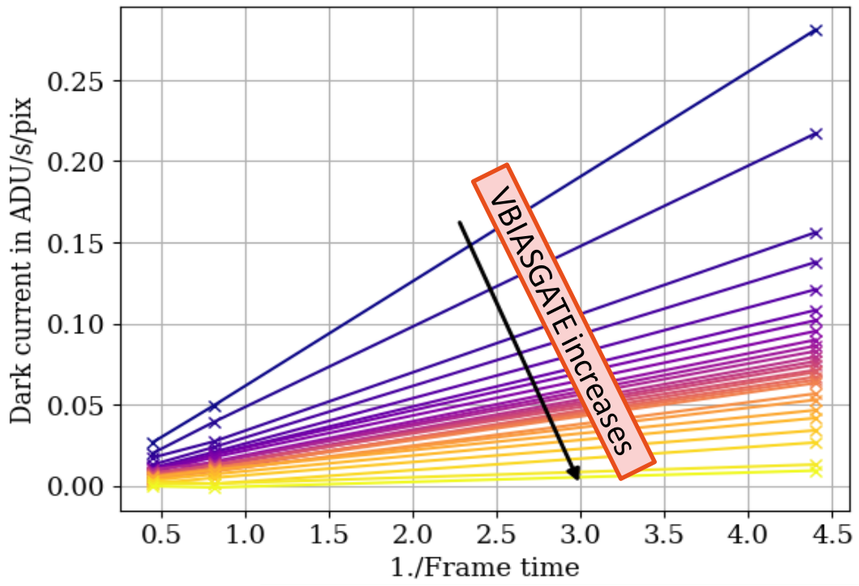

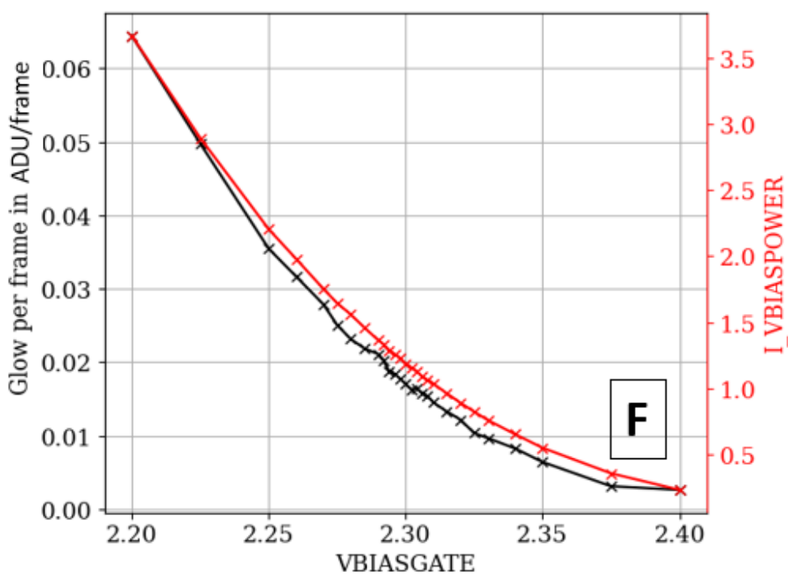

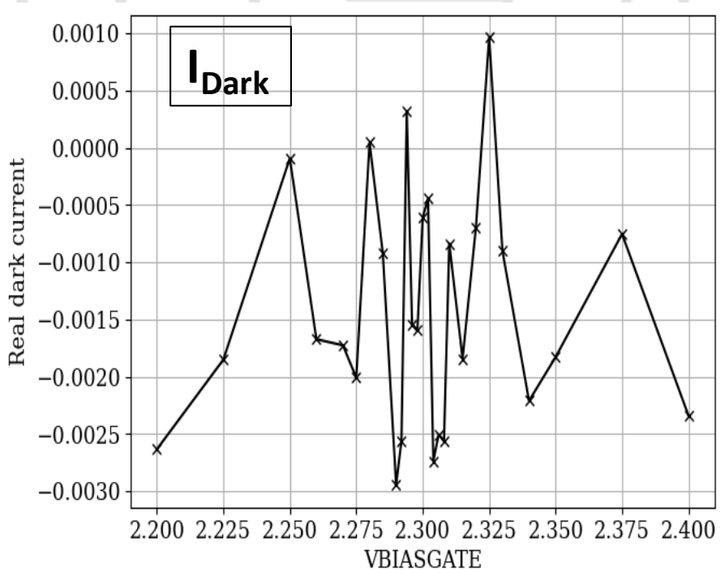

F ↘ when VBIASGATE ↗ (less current in the MOS of the pixel)

I_{Dark} close to 0 ADU/s

Strong correlation between F and VBIASPOWER current : *The greater the current in the MOS, the greater the contribution of the glow*

(2) M. W. Regan, L. E. Bergeron, "Zero dark current in H2RG detectors: it is all multiplexer glow", J. Astron. Telesc. Instrum. Syst. 6(1), 016001 (2020)

MWIR EM CH0 Detector

$T_{detector}$ @ 34K

	Measurement	T_{det}	Light source	Readout mode	Line	Col	Frame time	Measurement duration	t_{int}	N_{ramps}	N_{groups}
1.0	Glow t_f	T_1	None	FUR	355	64	**0.227**	1800	1800	1	7920
1.1	Glow t_f + 1.0	T_1	None	FUR	355	64	**1.227**	1800	1800	1	1467
1.2	Glow t_f + 2.0	T_1	None	FUR	355	64	**2.227**	1800	1800	1	808

$$S_{Dark} = I_{Dark} + \frac{F}{dt} \quad (2)$$

Effective dark current

Real dark current

Glow per frame

Frame time

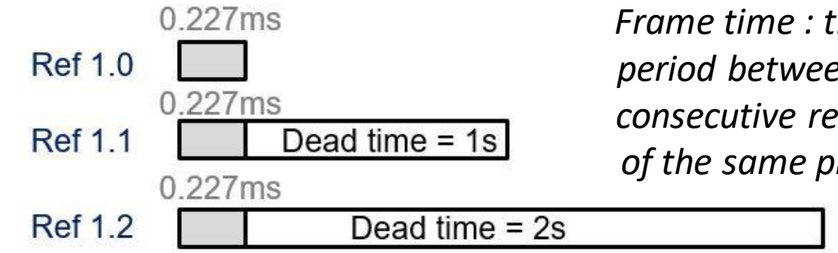

Frame time : time period between 2 consecutive reads of the same pixel

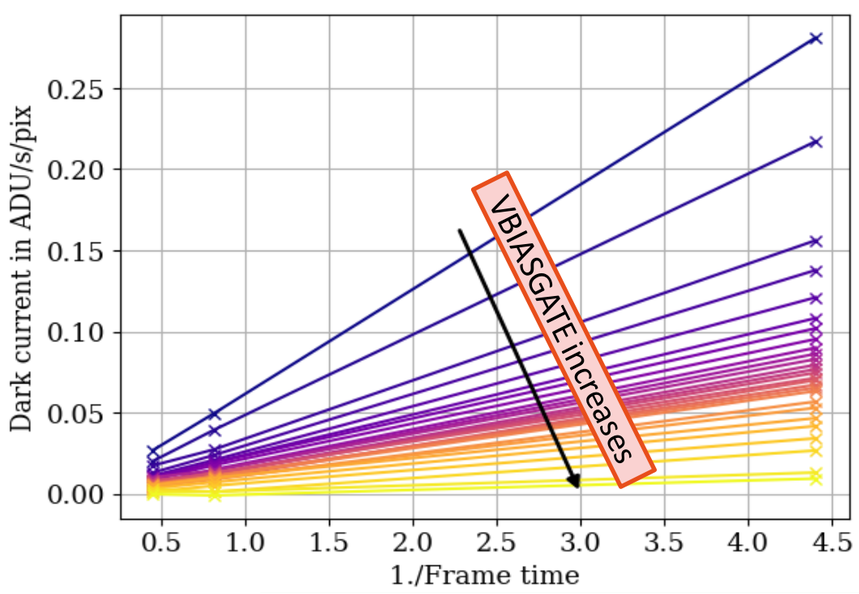

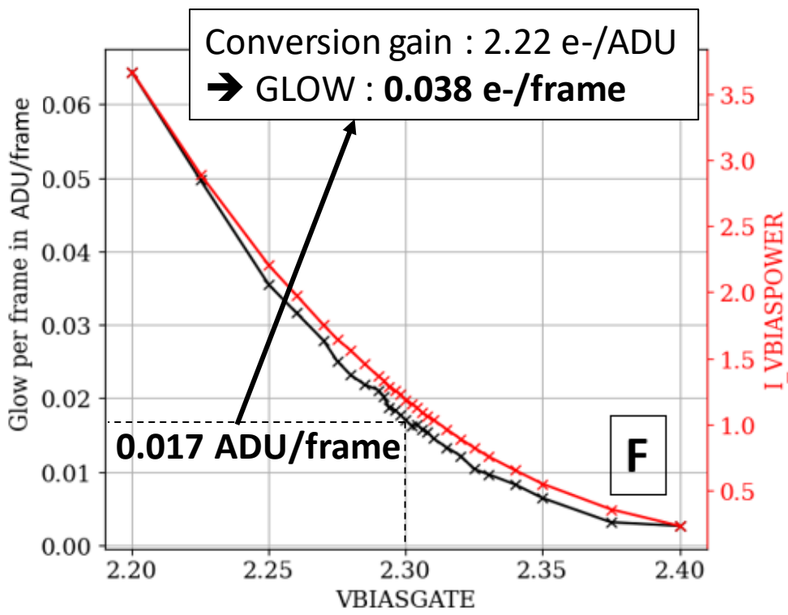

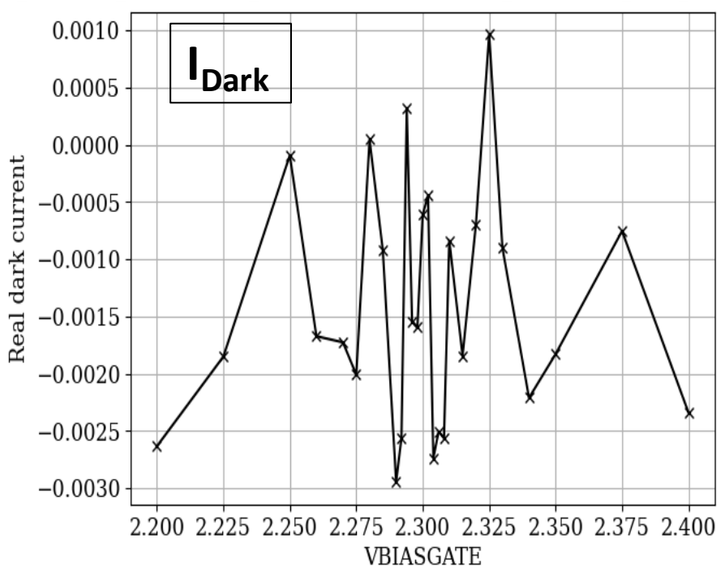

F ↘ when VBIASGATE ↗ (less current in the MOS of the pixel)

I_{Dark} close to 0 ADU/s

Strong correlation between F and VBIASPOWER current : *The greater the current in the MOS, the greater the contribution of the glow*

(2) M. W. Regan, L. E. Bergeron, "Zero dark current in H2RG detectors: it is all multiplexer glow", J. Astron. Telesc. Instrum. Syst. 6(1), 016001 (2020)

3. Characterization results
5. Study of readout glow

	EM CH0	EM CH1
Wavelength range	[0.4-4.75] µm	[0.4-8.09] µm
Glow per frame	0.038 e^-/frame	0.131 e^-/frame

Range ratio : 1.8
Glow per frame ratio : 3.4

3. Characterization results
5. Crosstalk estimation with hot pixels

Measurement realized in the dark. To estimate the crosstalk, the following steps are applied:

- ❑ Consider pixels with a high dark current (but not saturating)
- ❑ Keep only isolated hot pixels (5 pixels distance from other hot pixels)
- ❑ Compute the crosstalk coefficient α and the crosstalk kernel

$$\alpha_{CH0} = \frac{< N > - B_{median}}{C + 4 < N > -5B_{median}}$$

C: signal of the central pixel
$< N >$: mean signal of the 4 nearest neighbours
B_{median}: background signal of the pixels in the ROI

Measurement realized in the dark. To estimate the crosstalk, the following steps are applied:

- ❑ Consider pixels with a high dark current (but not saturating)
- ❑ Keep only isolated hot pixels (5 pixels distance from other hot pixels)
- ❑ Compute the crosstalk coefficient α and the crosstalk kernel

$$\alpha_{CH0} = \frac{< N > - B_{median}}{C + 4 < N > -5B_{median}}$$

C: signal of the central pixel
$< N >$: mean signal of the 4 nearest neighbours
B_{median}: background signal of the pixels in the ROI

Crosstalk kernel CH0

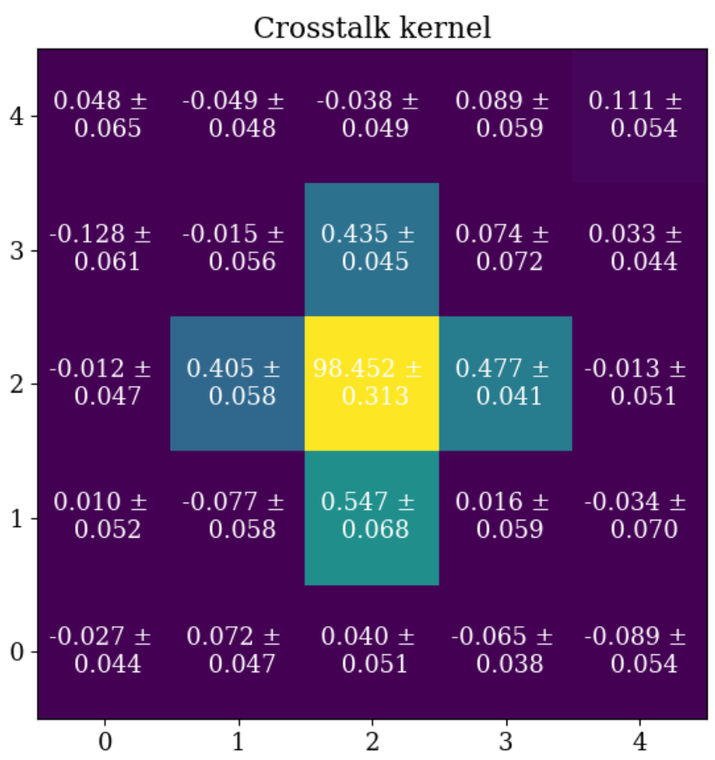

$\alpha_{CH0} = 0.5\%$

Crosstalk kernel CH1

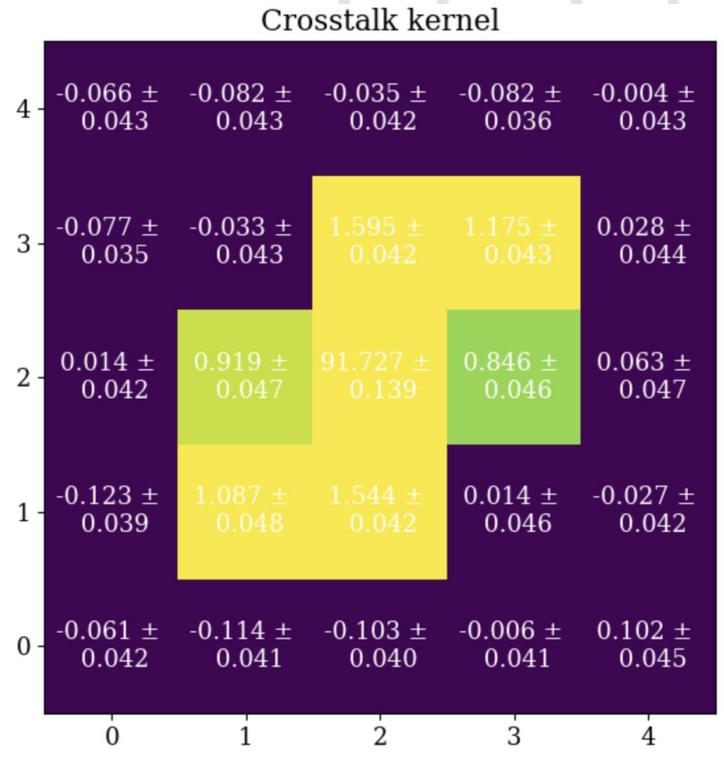

unexpected

$\alpha_{CH0} = 1\%$

3. Characterization results
6. Conversion Gain

Dataset : 100 different integration times considered, 100 ramps acquired for each integration time

Conversion gain measured with PTC technique:

Processing steps:

- ❑ CDS images built from these ramps, taking the difference between the first ant the last frame
- ❑ For each signal level, the mean and variance are computed for each pixel
- ❑ Perform chi-squared minimization to estimate the fitting parameter. A 3rd order polynomial function has been used to fit the PTC.
- ❑ The conversion gain (in e-/ADU) is taken as the inverse of 1st order coefficient of the fit

3. Characterization results
6. Conversion Gain

Dataset : 100 different integration times considered, 100 ramps acquired for each integration time

Conversion gain measured with PTC technique:

Processing steps:

- ❑ CDS images built from these ramps, taking the difference between the first ant the last frame
- ❑ For each signal level, the mean and variance are computed for each pixel
- ❑ Perform chi-squared minimization to estimate the fitting parameter. A 3rd order polynomial function has been used to fit the PTC.
- ❑ The conversion gain (in e-/ADU) is taken as the inverse of 1st order coefficient of the fit

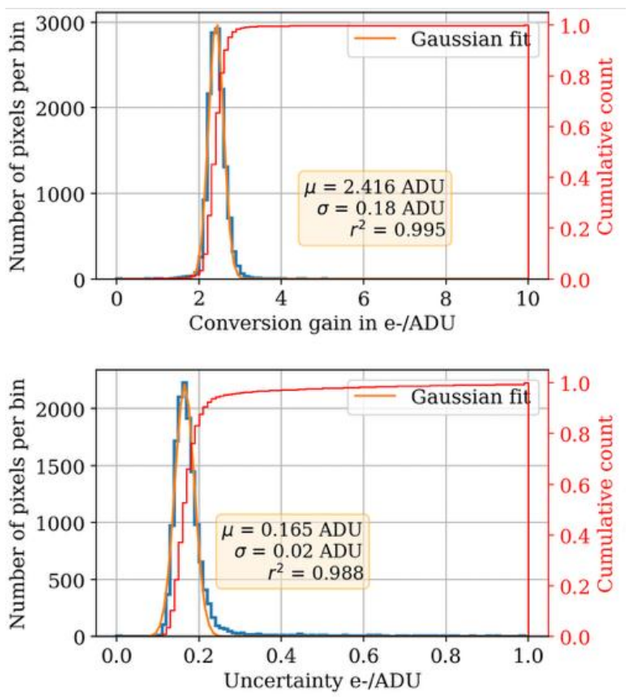

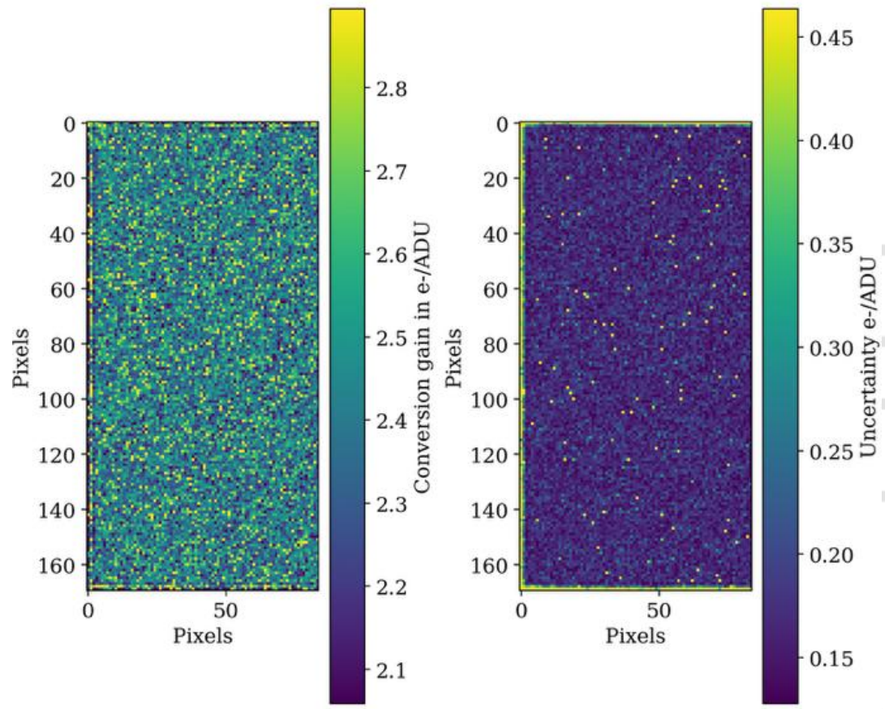

CH1: The conversion gain (not corrected for IPC) is equal to $g = 2.42 \pm 0.17\ e-/ADU$.
And **2.18 e-/ADU** when corrected by IPC.
CH0: 2.22 e-/ADU

3. Characterization results
6. Conversion Gain Stability

We are looking for very faint flux variation induced by transit over 10 hours (max), hence the conversion gain has to be stable.
➔ estimation of gain sensitivity in relation to detector temperature and biases applied to the detector (on going work)

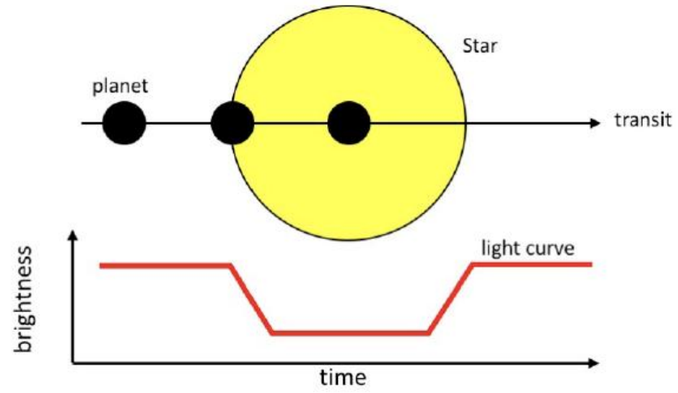

3. Characterization results
6. Conversion Gain Stability

We are looking for very faint flux variation induced by transit over 10 hours (max), hence the conversion gain has to be stable.
➔ estimation of gain sensitivity in relation to detector temperature and **biases applied to the detector** (on going work)

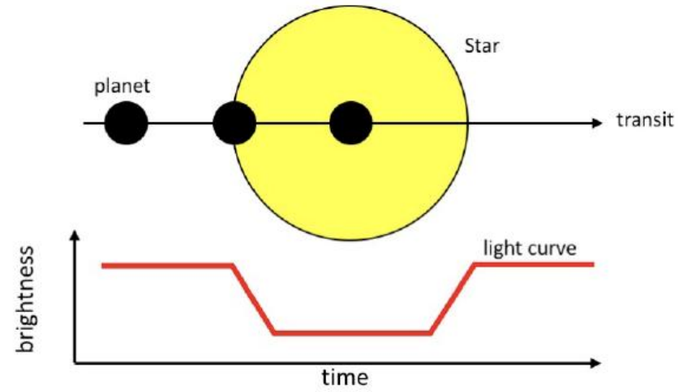

Conversion gain instabilities may arise from temperature variation of the warm electronics (Detector Control Unit)

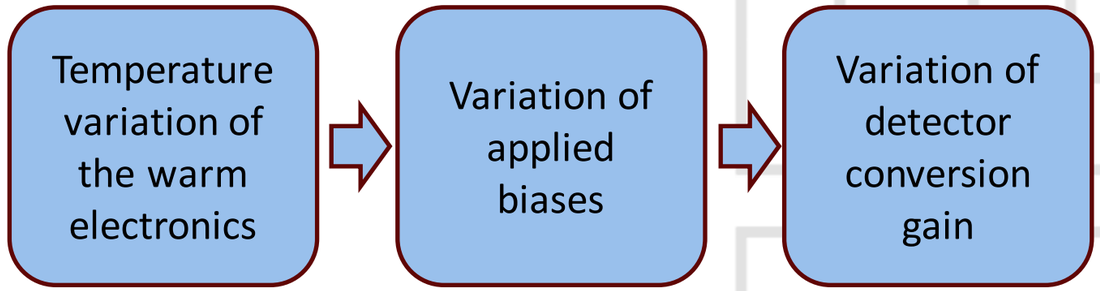

3. Characterization results
6. Conversion Gain Stability

We are looking for very faint flux variation induced by transit over 10 hours (max), hence the conversion gain has to be stable.
➔ estimation of gain sensitivity in relation to **detector temperature** and biases applied to the detector (on going work)

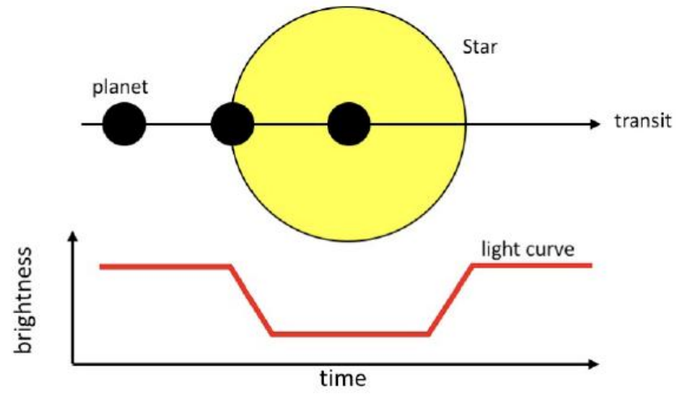

Evolution of the conversion gain as a function of CH1 detector temperature

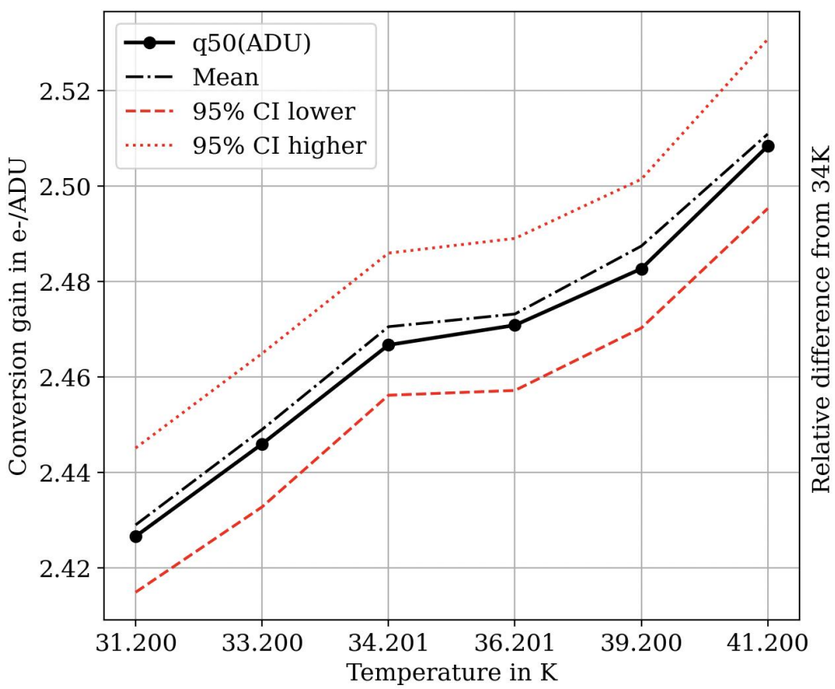

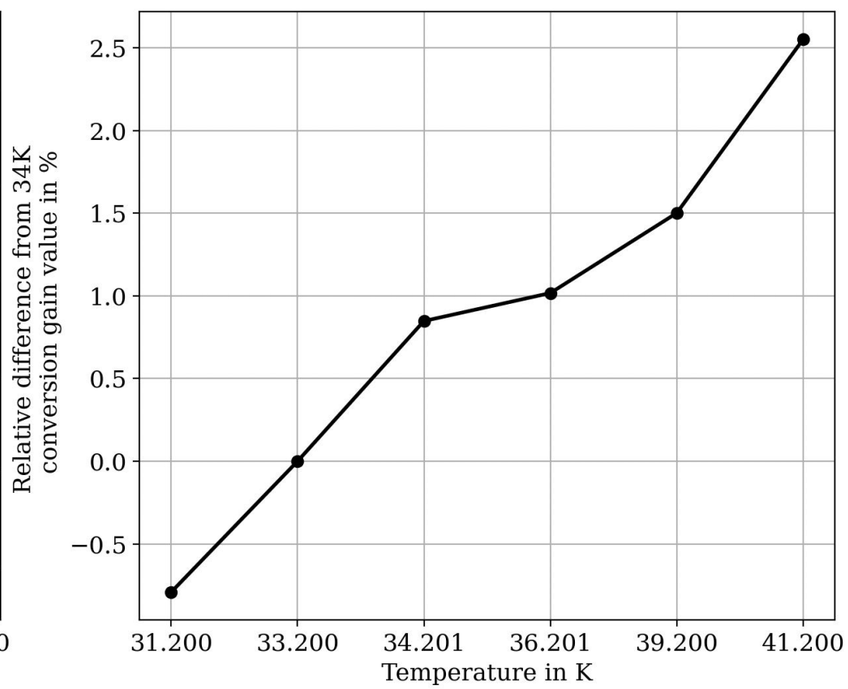

Conversion gain variation:
- ❑ **3.2 ppm/mK** (for CH1)
- ❑ **5 ppm/mK** (for CH0)

With a ±5mK thermal regulation, we ended up with a **25 ppm of variation** induced by the detector temperature variation *(for now, we have no physical explanation for this evolution)*

Plan

1. AIRS: ARIEL Infrared Spectrometer
    1. ARIEL space mission
    2. ARIEL spacecraft
    3. AIRS Acquisition chain architecture
2. Test bench at CEA
    1. Test bench presentation
3. Detector characterization results
    1. Strategy of calibration
    2. Detector baseline
    3. CDS and readout noise
    4. Dark current
    5. Readout glow
    6. Crosstalk
    7. Conversion gain and stability
4. Conclusion & Perspectives

Summary

- AIRS instrument composed of :
  - ❑ EM CH0 : [1.95-3.90] µm ➔ MWIR band
  - ❑ EM CH1 : [3.90-7.80] µm ➔ LWIR band

Summary

- AIRS instrument composed of :
  - ❑ EM CH0 : [1.95-3.90] µm ➔ MWIR band
  - ❑ EM CH1 : [3.90-7.80] µm ➔ LWIR band

Results :

- CDS noise : **13.25 electrons** (CH0) and **13.37 electrons** (CH1)
  - Compliant with AIRS specifications
- Dark current : **0.1 e^-/s/pix** (CH0) and **1.17 e^-/s/pix** (CH1)
  - Compliant to science needs
- Readout Glow : **0.038 e^-/frame** (CH0) and **0.131 e^-/frame** (CH1) ➔ variation with λ_c
- Median gain conversion : **2.22 e^-/ADU** (CH0) and **2.18 e^-/ADU** (CH1)
- Crosstalk : 0.5% (CH0) and 1% (CH1)

Summary

- AIRS instrument composed of :
  - ❑ EM CH0 : [1.95-3.90] µm ➔ MWIR band
  - ❑ EM CH1 : [3.90-7.80] µm ➔ LWIR band

Results :

- CDS noise : **13.25 electrons** (CH0) and **13.37 electrons** (CH1)
  - Compliant with AIRS specifications
- Dark current : **0.1 e^-/s/pix** (CH0) and **1.17 e^-/s/pix** (CH1)
  - Compliant to science needs
- Readout Glow : **0.038 e^-/frame** (CH0) and **0.131 e^-/frame** (CH1) ➔ variation with λ_c
- Median gain conversion : **2.22 e^-/ADU** (CH0) and **2.18 e^-/ADU** (CH1)
- Crosstalk : 0.5% (CH0) and 1% (CH1)

Unexpected Results :

- Difference in evolution of the baseline as function of biases for active pixels and reference pixels ➔ problem for reference pixel correction
- EM CH1 : Kernel Crosstalk ➔ diagonal variation observed
- Increase of the conversion gain with the detector temperature

Summary

- AIRS instrument composed of :
  - ❑ EM CH0 : [1.95-3.90] µm ➔ MWIR band
  - ❑ EM CH1 : [3.90-7.80] µm ➔ LWIR band

Test campaign during 1 year:
4.7 TB of data

Results :

- CDS noise : **13.25 electrons** (CH0) and **13.37 electrons** (CH1)
  - Compliant with AIRS specifications
- Dark current : **0.1 e^-/s/pix** (CH0) and **1.17 e^-/s/pix** (CH1)
  - Compliant to science needs
- Readout Glow : **0.038 e^-/frame** (CH0) and **0.131 e^-/frame** (CH1) ➔ variation with λ_c
- Median gain conversion : **2.22 e^-/ADU** (CH0) and **2.18 e^-/ADU** (CH1)
- Crosstalk : 0.5% (CH0) and 1% (CH1)

Test campaign @ LIRA, Meudon
Calibration of AIRS instrument

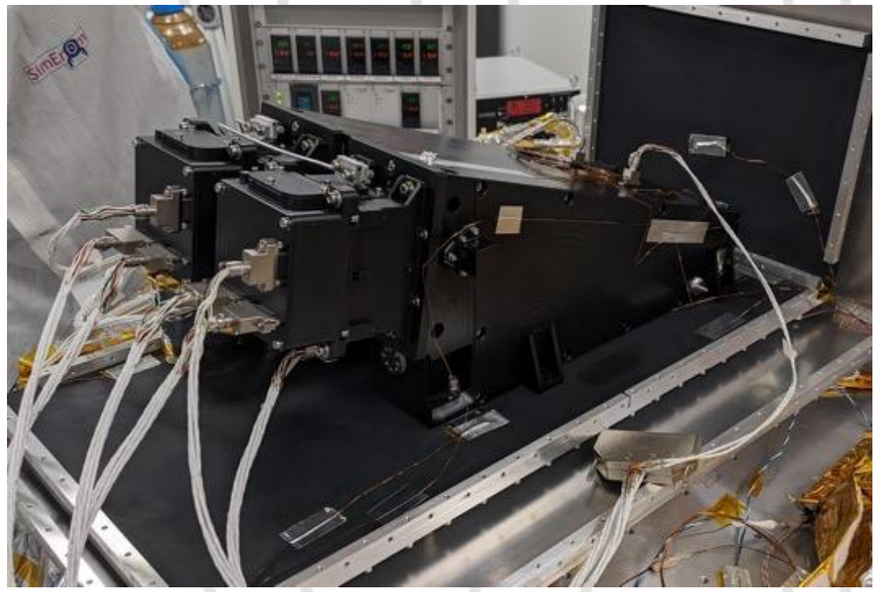

Unexpected Results :

- Difference in evolution of the baseline as function of biases for active pixels and reference pixels ➔ problem for reference pixel correction
- EM CH1 : Kernel Crosstalk ➔ diagonal variation observed
- Increase of the conversion gain with the detector temperature

AIRS is a joint development by :

1 hour-measurement in dark conditions ➔ 60 ramps of 60 seconds
1 hour-measurement under flux (1 ke-/s/pixel) ➔ 60 ramps of 60 seconds
1 hour-measurement in dark conditions ➔ 60 ramps of 60 seconds

EM CH0

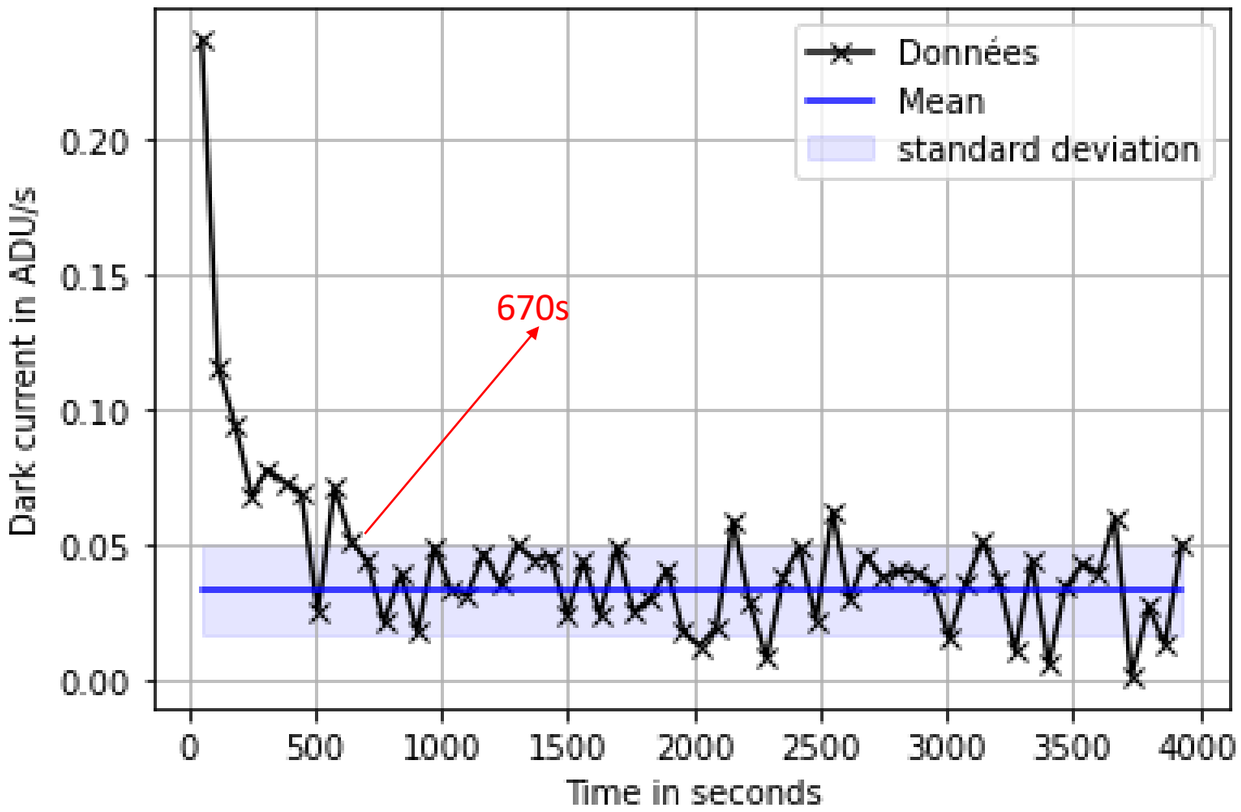

EM CH1

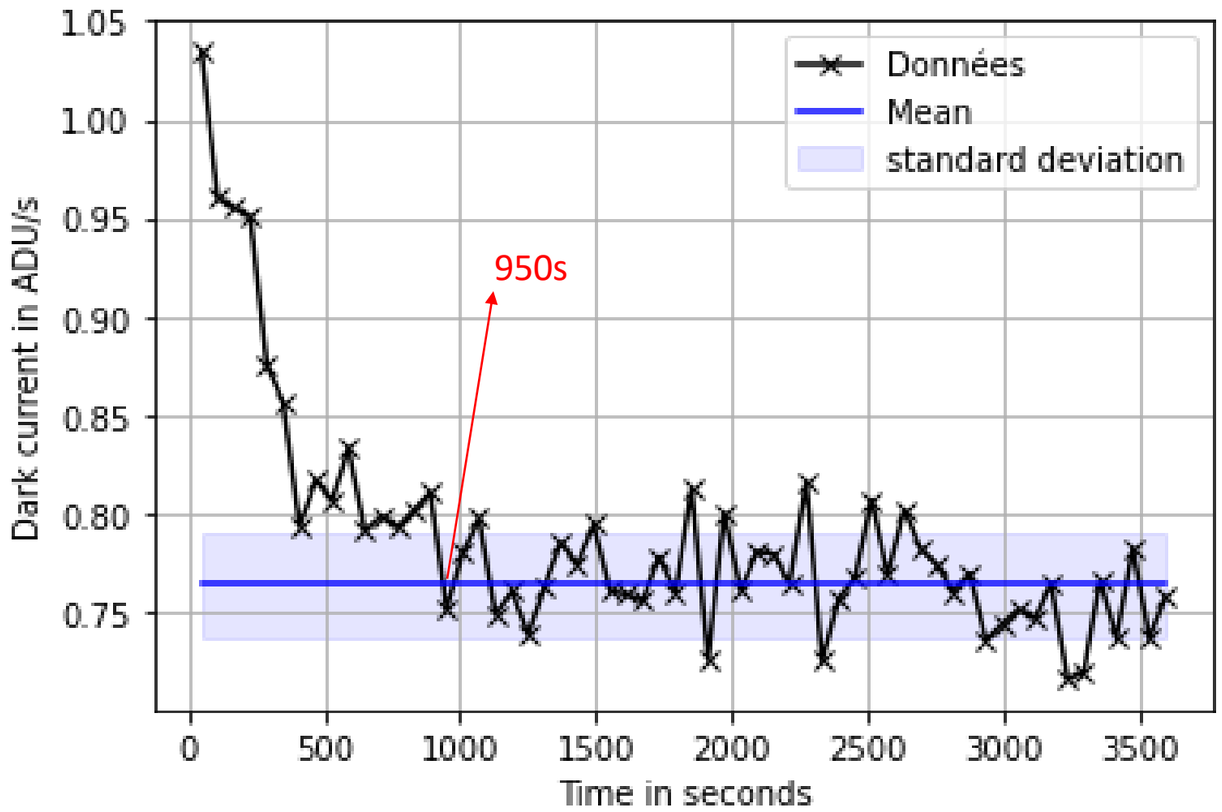

ANNEXE: EVOLUTION OF SIGNAL FOR REFERENCE PIXELS

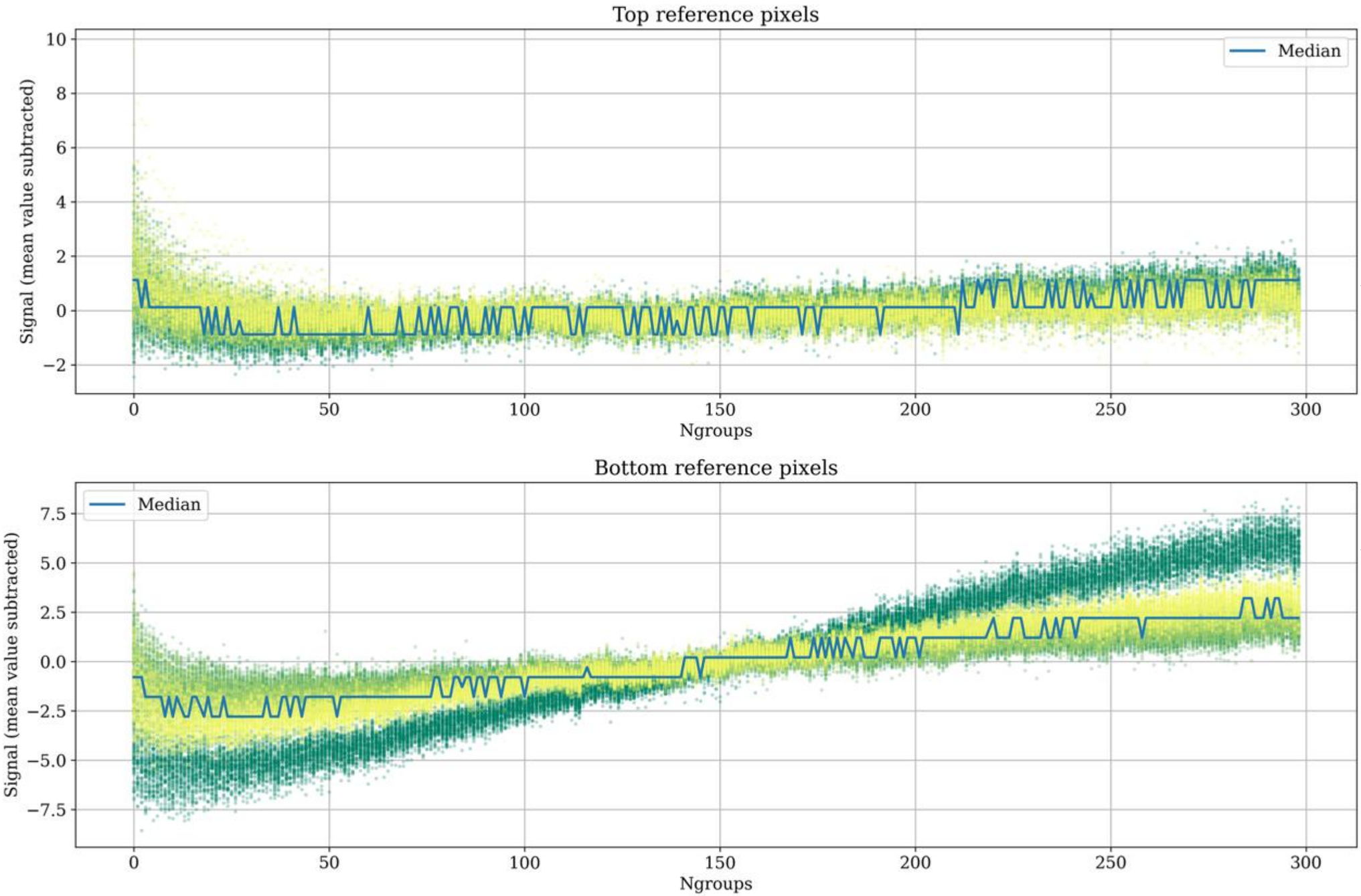

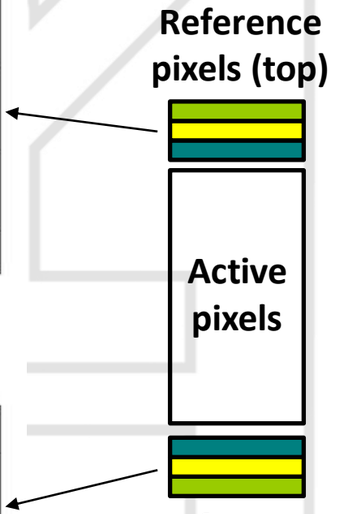

ANNEXE: STUDY OF THE READOUT GLOW FOR EM CH1 DETECTOR

$T_{detector}$ @ 34K

	Measurement	T_{det}	Light source	Readout mode	Line	Col	Frame time	Measurement duration	t_{int}	N_{ramps}	N_{groups}
1.0	Glow t_f	T_1	None	FUR	134	64	**0.9738**	1800	1800	1	18504
1.1	Glow t_f + 1.0	T_1	None	FUR	134	64	**1.9738**	1800	1800	1	1640
1.2	Glow t_f + 2.0	T_1	None	FUR	134	64	**2.9738**	1800	1800	1	858

VBIASGATE

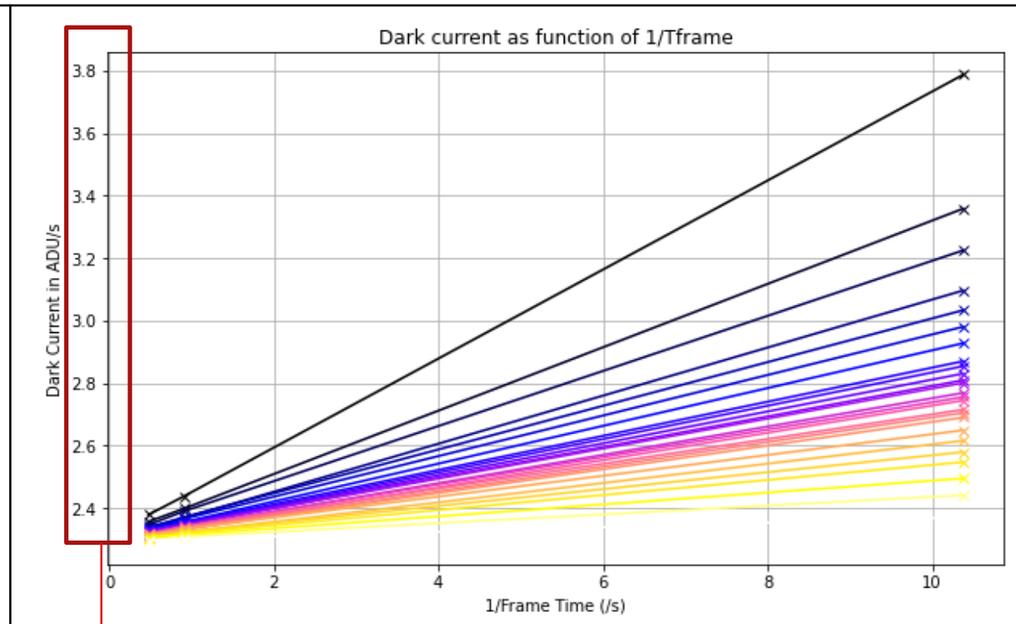

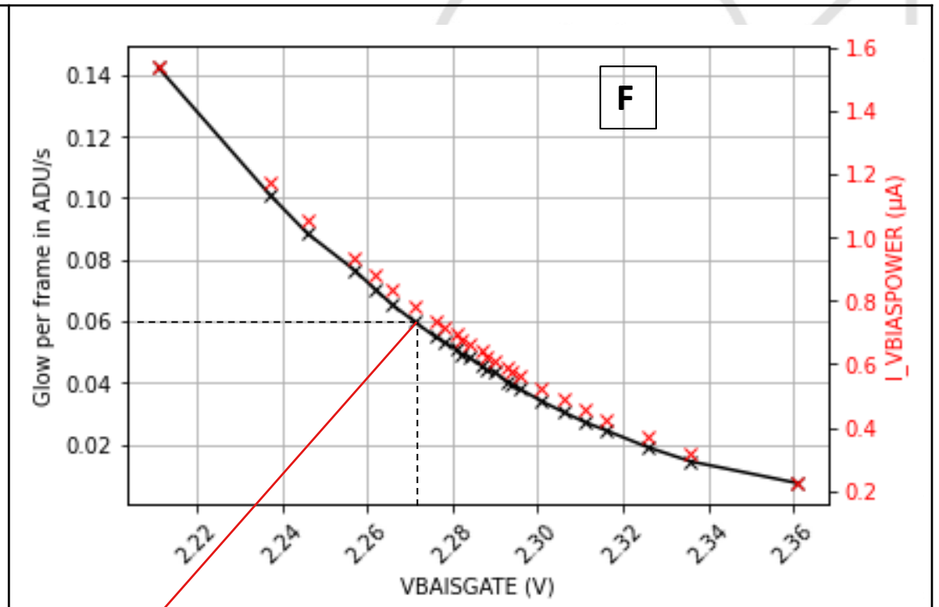

Light leak during the measurement

GLOW : 0.06 x 2.23 = **0.131 e-/frame**

Results consistent with T. Pichon and L.Boucher, « Pixel source follower glow in HxRG detector", Astronomische Nachrichten 344(8-9), e20230102 (2023)

≈ Detector temperature

= CFEE temperature

→ Detector baseline measurement

EM CH0

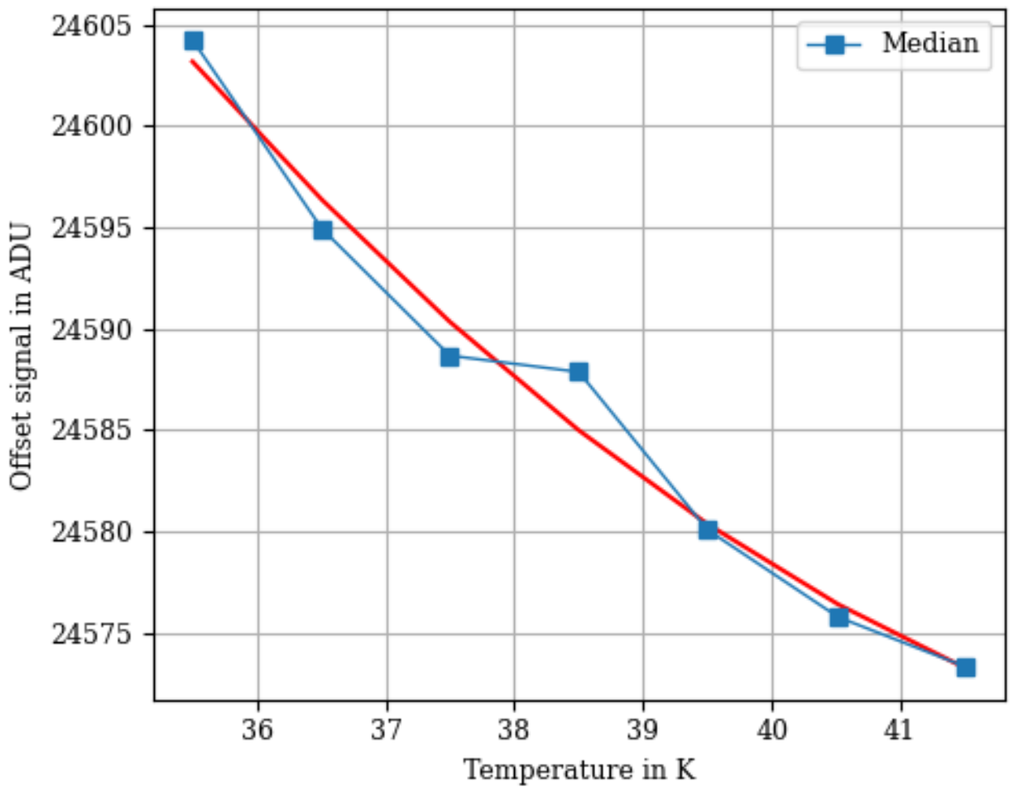

EM CH1

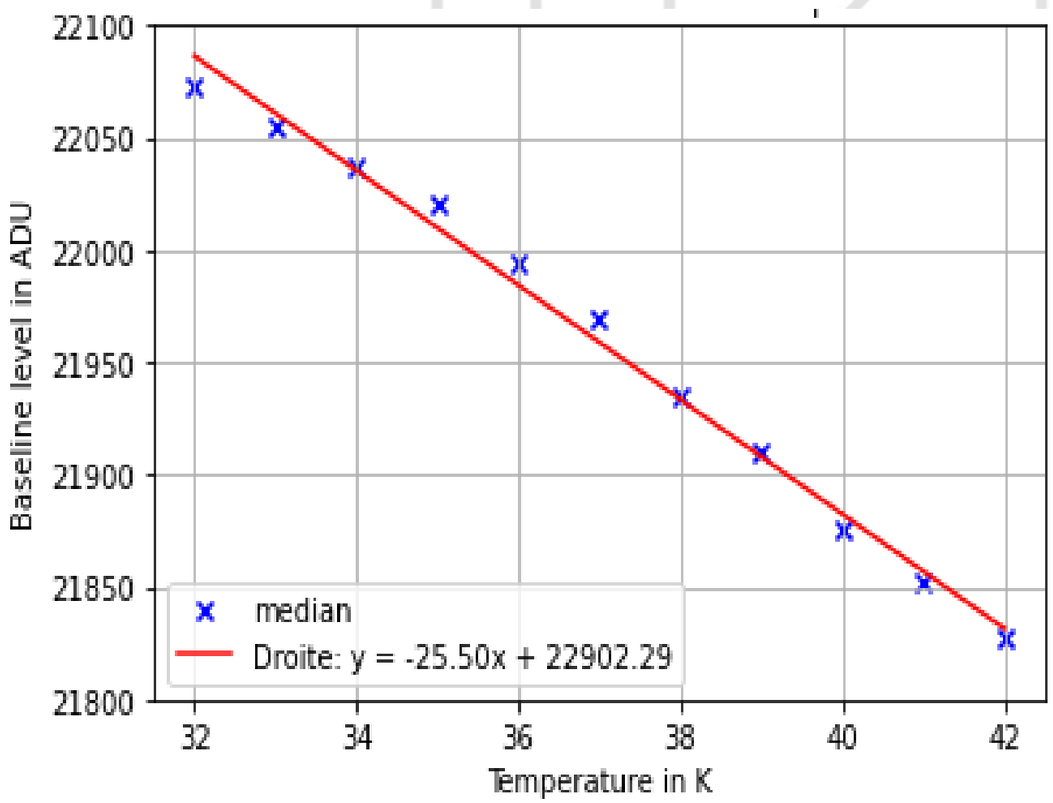

Small variation of the detector baseline with the detector temperature

ANNEXE: INFLUENCE OF THE TEMPERATURE

= Detector temperature

~ CFEE temperature

→ Detector baseline measurement

EM CH0

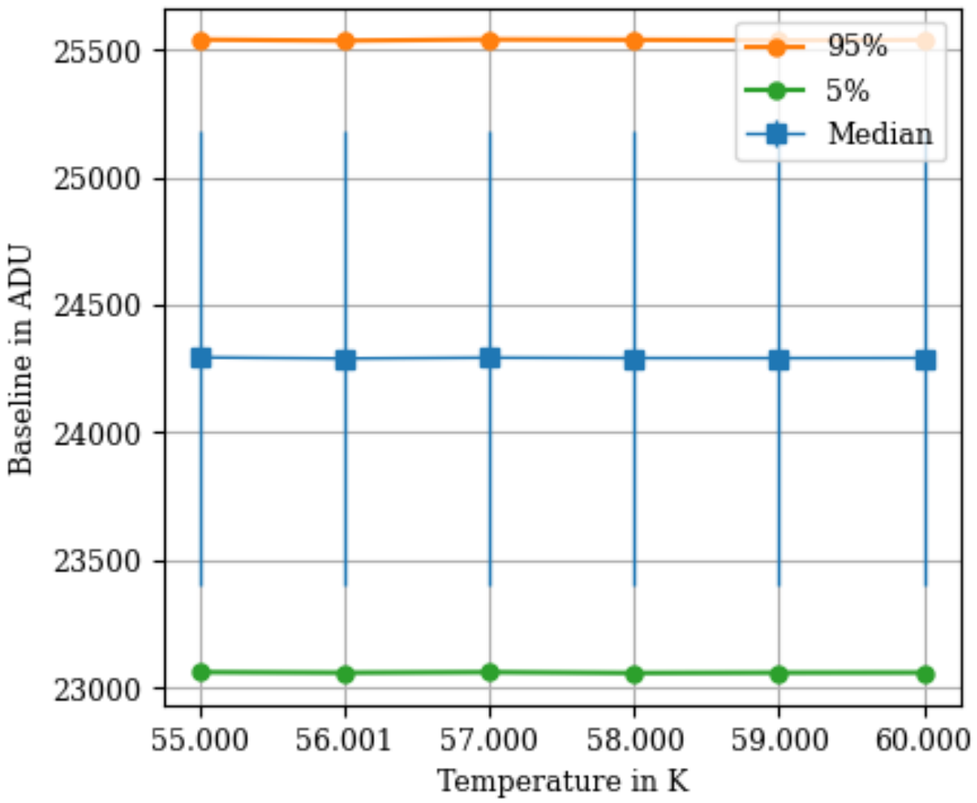

EM CH1

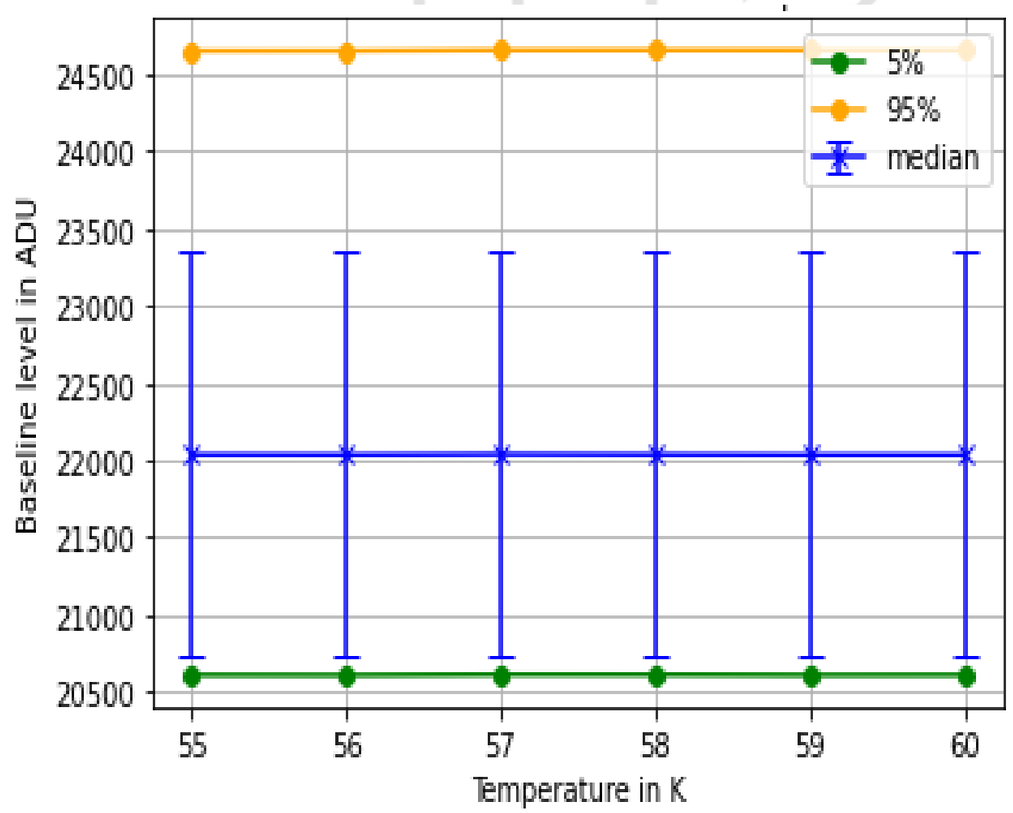

No influence of the CFEE temperature on the detector baseline

ANNEXE: WHAT ARE THE PHYSICAL PROCESSES INVOLVED ?

Excess of dark current from the collection by the photosensitive layer of the light emitted by the source follower transistor of a pixel

Light emission from the pixel SFD: electroluminescence

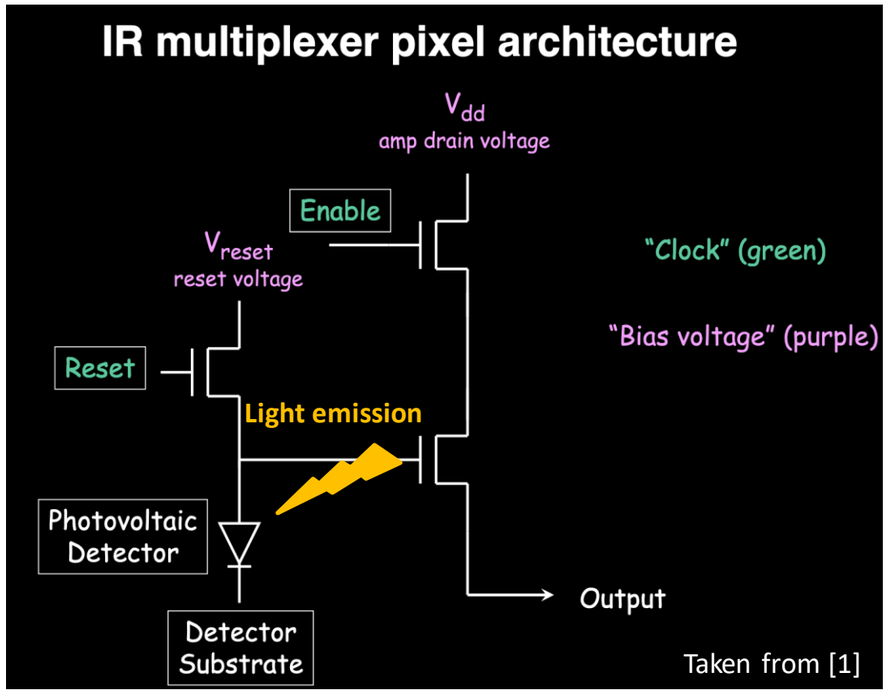

Each time the pixel is selected for read, light is emitted and adds up to real dark current.

Ligh emission by a MOSFET

$$N_{ph} = N_{e^-} \times P_{emission}$$

$$N_{ph} \propto A\frac{I_s}{q} \times (V_{ds} - V_{th})\exp^{-\frac{B}{V_{ds}-V_{th}}}\ [2]$$

- Is is the source current
- A, B account for MOSFET dimension, light extraction efficiency
- Vth threshold voltage

Two main options to reduce the glow:

1. Reduce the current flowing the SF transistor canal
2. Increase V_{ds} voltage (drain-source voltage) ➔ reduction

Of the electric field inside the detector's structure.

The more the pixel is selected, the greater the glow per frame.

[1] J.W. Beletic and L. Loose "Short Course detector for astronomy", (2009)
[2] F. Stellari, "Tools for non-invasive optical characterization of CMOS circuits", *IEDM Tech. Dig.*, 1999, pp. 487–490